

The Impact of Wildfire on Soil Erosion using a GIS-integrated RUSLE Model and the Influence
of DEM Resolution on Model Results

By

Amada Fernandez

A thesis submitted in partial fulfillment of the requirements
of the University Honors Program
University of South Florida, St. Petersburg

April 23, 2018

Thesis Director: Barnali Dixon, Ph.D.
Professor, College of Arts and Sciences

University Honors Program
University of South Florida
St. Petersburg, Florida

CERTIFICATE OF APPROVAL

Honors Thesis

This is to certify that the Honors Thesis of
Amada Fernandez
has been approved by the Examining Committee
on April 23, 2018
as satisfying the thesis requirement
of the University Honors Program

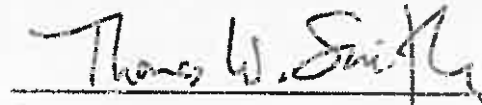
Examining Committee:

 5/3/18

Thesis Director: Bernali Dixon, Ph.D.
Professor, College of Arts and Sciences



Thesis Committee Member: Grant Steelman
Forestry Planner, Seminole Tribe of Florida



Thesis Committee Member: Thomas Smith, Ph.D.
Honors Program Director

Abstract

This study analyzes the environmental impact of wildfires on soil erosion in the surrounding watershed of the burn area. Depending on the severity and frequency, wildfires can have detrimental effects on the soils and hydrology of an ecosystem. Since severe wildfires alter the vegetation cover and the properties of the soil, researchers are often concerned with changes in sedimentation after a wildfire and its implications for watershed hydrology. Adverse changes to sedimentation can result in increases in surface runoff, soil erosion, sediment delivery to nearby streams, and peak flows. Assessing post-fire soil erosion risk is crucial in prioritizing watershed protection and mitigation efforts. A GIS-based model was used to estimate soil loss rates before and after California's 2010 Pozo fire. Rainfall erosivity, soil erodibility, conservation practice, topographic and land cover management factors before and after the fire were compiled in a GIS, where the Revised Universal Soil Loss Equation (RUSLE) was computed to estimate soil loss rates. Soil erosion values were classified into five erosion risk potential classes (low to high risk). Water quality data (TDS and TSS) for the Salinas watershed area was obtained from the EPA STORET Central Warehouse and used to determine the actual hydrological impact of the Pozo fire on the Salinas watershed and to verify RUSLE results. Percentage area of erosion 'hot spots' (moderately high to high risk) increased from 5.5% to 5.9% in the 30m and increased from 5.7% to 6.2% in the 90m model. These results indicate that the Pozo wildfire led to greater risk of erosion in the burn area. In the wet season before the fire (Dec 2009-Jan2010), 442 mg/l of TDS and TSS were found in the Salinas watershed, and 1,376 mg/l were found in the wet season directly after the fire (Dec 2010-Jan 2011). These results demonstrate that there was an increase in TDS and TSS downstream after the fire compared to before, and suggest that the Pozo fire is one plausible explanation for this increase. In addition, this study determined the impact of

digital elevation model (DEM) resolution on RUSLE results, as slope affects soil erosion and is represented in DEMs. The RUSLE model was run using 30m and 90m DEM resolutions for the topographic factor. The 30m model yielded maximum soil loss values of 341 tonnes ha⁻¹ yr⁻¹ for both pre- and post-fire models, while the 90m model yielded maximum soil loss values of 185 tonnes ha⁻¹ yr⁻¹ for the pre-fire run and 197 tonnes ha⁻¹ yr⁻¹ for the post-fire run, suggesting that soil erosion models using coarser resolution DEM data can underestimate maximum soil loss values.

1 Introduction

Wildfires can impact the hydrological system of the burn area both directly and indirectly. Wildfire has a direct effect on soils and hydrological systems through the burning of vegetation and its effect on landscape heterogeneity, followed by debris flow into nearby streams and rivers (Schoennagel et al. 2009). Loss in vegetation and litter cover can result in significant changes to rainwater interception, infiltration and evapotranspiration (Shakesby & Doerr 2006). Of concern to many researchers studying post-fire areas are the indirect effects including the effects on soil properties and the implications of vegetation cover changes on hydrological responses (Shakesby & Doerr 2006). Wildfire and its aftermath affect the way the burnt area and the surrounding watershed respond to rainfall, wind and other abiotic factors. In turn, these responses affect the ecological processes that follow the wildfire, such as the process of recovery and succession. The role of wildfire as an ecological determinant has been widely recognized, especially its role in the evolution of terrestrial ecosystems (Shakesby & Doerr 2006; Hoetzel et al. 2013). Certain terrestrial ecosystems and organisms have evolved to become dependent on wildfire for reproductive success, while others are more sensitive to fire (Mutch 1970). While wildfire can often result in a more heterogeneous landscape, ecosystem diversity and high

productivity, it can sometimes create the conditions necessary for damaging processes such as soil erosion and runoff. Thus, from an ecological perspective, wildfires can have both beneficial and adverse effects on a watershed's terrestrial and aquatic ecosystem. These impacts can have detrimental implications depending on both the severity of the fire and the system's response.

Understanding the environmental impact of wildfires on a watershed's downstream aquatic system has both ecological and anthropogenic benefits. Once the severity and environmental impact of a wildfire have been assessed by researchers, watershed mitigation efforts can be designed and executed to prevent severe land degradation (Vafeidis et al. 2007; Robichaud & Ashmun 2013). From an anthropogenic perspective, wildfires are often viewed as catastrophic events, especially when they occur at the wildland urban interface where development meets natural areas (Forrest & Harding 1994). These areas are of particular concern to officials, planners and the public because potential post-fire responses such as flooding, erosion or mudflow can be detrimental to public safety, private property and urban infrastructure (Robichaud & Ashmun 2013). Thus, assessing the environmental impact of wildfires near the wildland urban interface is crucial in limiting the hazardous impacts on human populations.

The research topic and study area chosen is further justified by recent events resulting from the 2017 California wildfire season. The 2017 season was the most disastrous on record. Induced by the California drought of 2011-2017, 9,000 wildfires burned an estimated 5,053 km² (CAL FIRE). Many of the fires took place at the wildland urban interface, resulting in \$180 billion in total damages and costs, including the destruction of neighborhoods, the closure of businesses and schools, fire extermination and rehabilitation costs (Accuweather 2017). The severe wildfire season has had other significant effects for residents of California. In one particularly severe case in Montecito, California (Santa Barbara County), a 200-year storm event

following a severe fire resulted in powerful flooding and mudslides. The flow of mud picked up debris and boulders, flowing at 35 to 50 miles per hour, and damaged the 101 Freeway, other roads, several homes, and resulting in at least 17 deaths (NBC 2018; NPR 2018). This event highlights the risk of mudslides and severe erosion events when heavy rainfall follows wildfires.

This thesis aims to analyze the impact of wildfire on hydrological systems, especially on the process of erosion and sediment transport to nearby streams and rivers and the downstream impact on aquatic systems. The Revised Universal Soil Loss Equation (RUSLE), a soil erosion model, was used to estimate soil erosion rates on a burnt plot of land before and after the fire event, and the model results for each condition were compared to determine the effect of the fire on erosion rates. In addition, this thesis addresses the impact of Digital Elevation Model (DEM) resolution on model results because the DEM is an important spatial input used in the soil erosion model. The results of this study and studies like it can be used by officials and planners to make decisions about post-fire watershed protection and mitigation efforts.

2 Literature Review

2.1 Hydrological Impact of Wildfires

2.1.1 Fire behavior

It has been demonstrated by many researchers that fire severity and intensity greatly affect the impact of the fire and the response of the affected ecosystem (Scott & Van Wyk 1990; De Luis et al. 2003; Doerr et al. 2006; Kokaly et al. 2007; Arcenegui et al. 2008). ‘Fire severity’ and ‘fire intensity’ are sometimes used interchangeably; however, the terms have distinct definitions. Fire intensity is the measurement of heat released per unit length of the fire front and can sometimes be estimated from the flame length (Doerr et al. 2006). Fire intensity is

influenced by fire temperature and fuel properties such as arrangement, fuel type, fuel moisture, weather conditions and the presence of oils and resins in the fuel (DeBano et al. 1998).

Fire severity has a slightly more subjective meaning, as it qualitatively describes the ecological responses to the fire, of which there are many. The severity of the fire is dependent on fire behaviors such as intensity and duration of the fire as well as the characteristics of the burn area such as fuel type, vegetation cover, terrain and soil characteristics (Shakesby & Doerr 2006). Fire severity is classified as low, moderate or high and is usually based on observations and measurements of the effect of the fire on soils, vegetation and hydrological systems (Hartford and Frandsen 1992). See Appendix A for a severity map of the Pozo fire.

In general, as fire severity increases, the severity of the effect on the terrestrial and nearby aquatic ecosystems also increases. Low severity fires have little to no impact on soil properties due to lower temperatures. As soil temperatures increase with fire severity, soil aggregate stability and porosity decreases, making soil more vulnerable to detachment by raindrop impact or to sediment transport by surface runoff (DeBano et al. 1998; Shakesby & Doerr 2006). In addition, as fire severity increases, the amount of burned or removed green vegetation, litter and ground/shrub fuel also increases. The removal of or burning of vegetation in higher severity fires also has implications regarding soil erosion after wildfire, since vegetation provides interception to protect against raindrop impact and because vegetation and its roots can store water near the surface, which can mitigate surface runoff which can carry with it detached sediments to nearby aquatic systems (Kutiel et al. 1995; DeBano et al. 1998; Mallinis et al. 2009).

Because fire intensity and severity depend on many fuel properties, it is difficult to create a general description of severity thresholds and parameters for all wildfires. Table 1

demonstrates the relationship between fire severity classification, fire intensity, post-fire conditions and the environmental impact for eucalypt-dominated forest, which is used as an exemplar (Byram 1959; DeBano et al. 1998; Shakesby et al. 2003; Shakesby & Doerr. 2006).

Table 1. Fire severity and intensity parameters. Modified from Cheney (1981).

Fire severity (Cheney 1981)	Fire intensity (kW m^{-1}) (Byram 1959)	Maximum flame height (m) (Cheney 1981)	Post-fire conditions	Environmental impact
Low	<500	1.5	Vegetation <2 m is burnt, others unburnt. Litter and duff layers are scorched but entire depth is not affected. Mineral soil is unchanged. Soils at 1 cm are less than 50°C. Surface is black and may contain grey ash (DeBano et al. 1998)	Little to no impact on soil properties, infiltration, runoff, erosion and quality of nearby bodies of water because of low temperatures and unchanged soils. Infiltration rates measured between 60-80 mm h^{-1} (Robichaud 2000). Low severity fires may stimulate plant reproduction for some species and may return nutrients to soil.
Moderate	501-3,000	5.0	Vegetation <4 m is burnt, including all ground and shrub fuel. Moderate soil heating occurs, litter is consumed, duff is charred, but mineral soil is not altered. Soils at 1 cm are between 50°C and 200°C and surface may contain light ash (DeBano et al. 1998).	Little to no impact on soil properties including soil aggregates because soils are not heated enough at the moderate severity level to affect soil structure/chemistry. Burning of ground and shrub fuel may result in moderate decreases in infiltration and increases in surface runoff. Infiltration rates measured between 30-84 mm h^{-1} (Robichaud 2000).
High	3,001-7,000	10.0	Vegetation <10 m is burnt, including all ground and shrub fuel and some lower canopy. High soil heating occurs, litter and duff are consumed, mineral soil is altered and soils at 1 cm are between	When soil temperatures reach the high end (>220°C) of this range, moderate impacts on soil properties may occur including the reduced stability and porosity of soil aggregates, which may result in reduced infiltration rates and increased

			200°C and 250°C (DeBano et al. 1998).	water repellency and surface runoff. Infiltration rates measured between 23 and 55 mm h ⁻¹ (Robichaud 2000).
Very high	7,001-70,000	10-30	All green vegetation <30 m is consumed as well as woody fuels with diameter <5 mm. High soil heating occurs, litter and duff are consumed, mineral soil is red or orange and soils at 1 cm are greater than 250°C (DeBano et al. 1998).	Soil temperatures at this level often result in the reduction of soil aggregate stability and porosity, resulting in reduced filtration rates and increased water repellency and surface runoff. Infiltration rates are measured greater than 55 mm h ⁻¹ (Robichaud 2000). The greater loss of vegetation at this stage has greater impacts regarding reduced interception of precipitation and increased vulnerability to sediment detachment and transportation by water, leading to greater risk of erosion.
Extreme	>70,000	20-40	All green vegetation is consumed as well as woody fuels with diameter <10 mm. High soil heating occurs, litter and duff are consumed, soils at 1 cm are greater than 250°C and may be dark or charred up to 10 cm (DeBano et al. 1998).	Extremely high soil temperatures at this level reduce soil aggregate stability and porosity, resulting in reduced filtration rates and increased water repellency and surface runoff. Infiltration rates are measured greater than 55 mm h ⁻¹ (Robichaud 2000). The complete removal of green vegetation at this stage has great impacts regarding reduced interception of precipitation and increased vulnerability to sediment detachment and transportation by water, leading to extreme risk of erosion.

In addition, duration of the fire and rate of spread have a significant influence on the severity of the fire and the ecosystem's response. Rate of spread has the greatest impact on belowground damage. Fast-moving fires may release great amounts of energy per unit area and

thus have a high intensity, but they may not have sufficient time to transfer heat to soils (DeBano et al. 1998). Therefore, a fast-moving fire may not result in increased risk of soil erosion due to the lack of heat transfer to soils, which makes the soils less vulnerable to detachment. Slow-moving wildfires, regardless of intensity, are more damaging to belowground systems and soils, especially in forests with heavier fuels. In the case of a slow-moving fire which may damage soils more than a fast-moving soil and which may burn more vegetation, greater increases in erosion risk can be expected. Effects of wildfire on belowground systems and soils are of particular interest in studies of the hydrological impacts of fires because belowground systems and soils play a large role in hydrological and erosional processes (Neary et al. 1999).

Weather conditions following the fire, including the presence, absence, amount and intensity of precipitation, greatly impact hydrological and sediment processes. Absence of precipitation for some time following a fire of any severity or intensity may result in minimal hydrological and sedimentary responses. Conversely, precipitation following a slow-moving or high severity fire can have detrimental impacts on the hydrological and sedimentary responses, possibly resulting in increased surface runoff, peak flows and sediment delivery to nearby streams (Neary et al. 1999). Of particular concern is the quantity and intensity of the precipitation, as well as the time since the fire. Heavy rains only a few days after a fire may result in more adverse effects than light rains a few days after a fire or heavy rains months after a fire.

2.1.2 Vegetation

The most direct effect of wildfire is that of vegetation cover changes, as litter and vegetation may be removed by the fire. The extent to which litter and vegetation are removed

depends on the severity of the fire. Low severity fires are more likely to burn the surface (vegetation), while high intensity/severity fires are more likely to burn the ground. Removal of vegetation reduces the amount and rate of evapotranspiration of the affected area. Depending on the volume of vegetation burned, this may or may not have a significant effect on the hydrological cycle of the system (Morton 1983; Zhou et al. 2013). Vegetation and its roots directly affect the amount of water that can be stored on the surface. Thus, a reduction in vegetation would result in a reduction in the amount of water storage available on the surface. By burning vegetation, wildfires alter the landscape cover heterogeneity. Fire-induced changes to surface heterogeneity greatly influences the rate of erosion and runoff generation (Kutiel et al. 1995; Mallinis et al. 2009). In undisturbed forests, vegetation canopies and litter typically intercept precipitation as it falls toward the ground. By dissipating the energy of the falling raindrops, vegetation canopies and litter accumulation play an important role in protecting soils from raindrop impact, which can compact or dislodge soil particles, in turn affecting the infiltration rate of the soil (DeBano et al. 1998; Zhang et al. 2009). Exposed soils can result in increased water repellency in soils, which can lead to more serious processes such as soil erosion or surface runoff (Wondzell 2001; Doerr et al. 2006).

2.1.3 Soil biota

Depending on the type (ground, surface and crown) and intensity of the fire (the degree to which the soils are heated), soil biota populations living in the top centimeters of the soil are often reduced. Fire-induced soil biota changes are most sensitive to soil heating, and mortality of soil-dwelling fauna typically occurs when soils reach about 200 °C. In some cases, microbial populations can quickly recover to pre-fire numbers (Neary et al. 1999). When this is not the case, the reduction in soil biota can have indirect effects on the system's hydrology. Microbes

living in the top layer of the soil produce cohesive mucus, and fungi produce fungal hyphae that stabilize and protect soils against erosion (Shakesby & Doerr 2006). In their temporary fire-induced absence, soils become more susceptible to erodibility. In addition to microbes and fungi, soil invertebrates such as insects may suffer population reductions after a wildfire. These invertebrates typically facilitate water infiltration by creating small arteries through which water can penetrate and flow. When soil-dwelling invertebrate populations suffer significant reductions, reduced infiltration may contribute to increased surface runoff (Shakesby & Doerr 2006). Soil biota additionally contribute to the mixing and transfer of sediment called bioturbation. One type of bioturbation, sediment bio-transfer, is of particular significance in the study of the hydrological impacts of wildfire. Sediment bio-transfer involves the direct downslope movement of sediment by soil-dwelling biota. When soil-dwelling fauna in vulnerable post-fire soils loosen sediment particles through bioturbation, risk of increased sediment transfer by overland flow becomes significant (Dragovich & Morris 2002).

2.1.4 Soil properties

The effect of fire on soil aggregate stability is dependent on the fire temperature, fire duration and soil characteristics (DeBano et al. 1998; Guerrero et al. 2001; Huffman et al. 2001). Because aggregation influences soil's susceptibility to erosion, plant growth and the entry and movement of water, fire-induced reductions in soil aggregate stability can have widespread effects on hydrology. Aggregate stability describes the pore space and binding between soil aggregates and the resistance to disturbance, mostly by water (Amezketta 1999). Soil aggregate stability is naturally low in some soil types, such as sandy soils, because the soil properties allow water and plant roots to move without difficulty. However, soil aggregate stability is more

important for other soil types, in which case large pores between soil aggregates are most desirable to allow for greater water entry and movement. Soil aggregates that are more stable are more protected against raindrop impact, which can dismember soil particles, clogging pores and creating a crusty surface. Fire affects soil aggregate stability when heating exceeds 220-460 °C. At these temperatures, organic matter is combusted and hydroxyl groups may be driven off, altering the structure of the soil aggregates (DeBano et al. 1998; Shakesby & Doerr 2006). Soils with reduced soil aggregate stability and porosity in severely burnt areas may result in a more water-repellent surface that reduces soil permeability up to 6-8 cm from the surface (Henderson & Golding 1983).

2.1.5 Infiltration

The effect of wildfire on infiltration is an indirect effect since it depends on fire-induced disturbances such as changes to soil aggregation, changes to vegetation cover, fire severity and post-fire precipitation conditions such as rainfall intensity and frequency (Wondzell 2001). Most studies examining the effect of wildfire on infiltration have found a decrease in infiltration rates in recently and severely burnt areas (Imeson et al. 1992; Kutiel et al. 1995; Wondzell 2001; Cerdà & Robichaud 2009; Robichaud & Ashmun 2013). Robichaud (2000) studied the effect of fire severity on infiltration rates by performing simulated rainfall events on prescribed burn sites. It was found that as fire severity increased, infiltration rates decreased. Infiltration rates were measured to be between 60 and 80 mm h⁻¹ for low intensity fires, 30 and 84 mm h⁻¹ for medium intensity fires, and 23 and 55 mm h⁻¹ for high intensity fires.

Infiltration is defined as the movement of water in the soil, influenced primarily by rainfall intensity and soil properties such as soil aggregate stability and water repellency (Cerdà

& Robichaud 2009). During a rain event, the rate of infiltration increases initially until it reaches a constant, typically after several minutes, at which point the water that does not infiltrate the soil becomes surface runoff (Dunin 1976). Because rate of infiltration is partially a function of vegetation cover and soil properties, changes to these parameters due to fire disturbances often result in infiltration rate reductions (Cerdà & Robichaud 2009). Vegetation on the forest floor serves as both a water storage and a rainfall interception that can reduce rainfall impact and aid in the infiltration of rainwater into the soil surface. In addition, plant roots that penetrate into the soil increase soil porosity, improving infiltration rates. Depending on fire severity, wildfires can cause great damage to vegetation and litter cover, eliminating some of the water storage capacity and rainfall interception (Summerfield 1991). Additionally, changes to the soil properties, discussed in the previous subsection, often lead to soil water repellency that results in infiltration reductions. Decreases in infiltration rates lead to increases in surface runoff, which can result in increased erosion processes and streamflow. Post-fire infiltration rates typically improve after vegetation cover is re-established, which may take several months to a few years (Cerdà & Robichaud 2009).

2.1.6 Surface runoff

Surface runoff, also called overland flow, can occur by saturation overland flow or by infiltration-excess overland flow. Saturation overland flow occurs when the soil becomes saturated due to prolonged rainfall. The water that is not infiltrated into the soil after it has reached its saturation point becomes surface runoff. Infiltration-excess overland flow occurs when the rate of rainfall or water input exceeds the infiltration rate ability of the soil (Smith and Goodrich 2006). Most researchers attribute post-fire surface runoff to infiltration-excess

overland flow rather than saturation overland flow due to common post-fire reductions in soil wettability, which lowers the infiltration rate ability of the soil (Shakesby & Doerr 2006). Thus, like post-fire infiltration trends, wildfire-induced surface runoff is an indirect effect and is a function of the fire severity, the damage to the vegetation cover and to soil aggregate stability. For example, Benavides-Solorio and MacDonald (2001) applied artificial storms of 80 mm h^{-1} on unburnt plots and recently burned plots of varying severities in an attempt to understand the impact of burn severity, percent ground cover, soil repellency and time since burning on the magnitude of post-fire surface runoff and sediment yield increases. The most severely and recently burned plots yielded runoff ratios 15-30% greater, as well as sediment yields 10-26 times greater, than unburned or low severity fires. Plots burned more than five years before the experiment experienced only slightly more runoff or sediment yield than unburned plots, and 81% of the variability in sediment yield was attributed to percent ground cover, which explains why the plots burned over five years before the experiment behaved more similarly to unburned plots.

Most study results have found that the greatest impact of wildfire on surface runoff occurs during rain events directly following the fire, and that as vegetation recovers over time and soil properties return to pre-fire conditions, rain events have lesser impact on the surface runoff of the burn area (Doerr et al. 2006). In addition, most agree that the rainfall intensity and frequency after the fire must be relatively high to produce significant surface runoff. For example, Prosser and Williams (1998) compared runoff and erosion between burnt and unburnt sites after the 1994 fire in *Eucalyptus* forests surrounding Sydney, Australia. While burnt plots experienced greater runoff than unburnt plots, they reported that only rainfall events of greater than one-year recurrence yielded significant runoff and erosion. Since the year 1994 was

unusually dry, concerns of increased soil erosion due to post-fire runoff were not realized.

Therefore, the local climate is an important aspect for researchers to consider when examining post-fire environmental impacts. Researchers studying an area with little annual rainfall might be less concerned with increases in surface runoff due to wildfire than those studying areas with abundant annual rainfall. Instead, in drier areas, researchers might focus on other impacts of wildfire such as damage to vegetation and soil properties and the possibility of increased wind erosion.

2.1.7 Erosion

The possibility of post-fire accelerated soil erosion by water is a function of the previously discussed effects of wildfire on components of the affected ecosystem. For example, changes to vegetation due to fire is the primary factor affecting post-fire soil erosion rates, since vegetation typically provides a canopy that protects soil from direct raindrop impact (Zhang et al. 2009). In addition, removal of or damage to a forest's duff layer leaves soils further exposed to raindrop impact during a rain event after the fire, since the duff layer is essential in the infiltration of water, and it elongates flow paths (Robichaud and Miller 1999). When soils are directly exposed to raindrop impact due to destruction of both of these protective layers, precipitation (depending on the severity and duration) can impair soil aggregate stability, detaching sediment. When sediment is detached and moved a short distance, simply redistributed on the soil surface, the process is called interrill or sheet erosion. Rill erosion occurs when fire-induced decreases in soil permeability and infiltration rates result in increases in surface runoff, which carries the detached sediment downhill to nearby streams and channels (Miller et al. 2016). In this way, all of the possible direct and indirect effects of wildfire can contribute to

result in the possibility of increased or accelerated soil erosion in burnt plots. In general, researchers and modellers assessing the impact of a fire on the soil and hydrology are concerned with rill erosion, since it involves the transportation of sediment by water to nearby channels and streams.

2.1.8 Water Quality

When soil particles are detached and carried by surface runoff, they are likely to be transported to nearby streams or rivers. Sediment transport is the movement of soil particles by water. Once sediment flows through a body of water, it may settle at the bottom of the body of water, resulting in deposition (DeBano et al. 1998). Although the soil erosion model used in this study cannot predict the sediment transport or deposition induced by fire, the hydrological impact of the fire can be directly obtained by water quality data available through the U.S. Environmental Protection Agency (EPA). Total suspended solids(TSS) and total dissolved solids (TDS) found in the water are indicators of soil erosion in surrounding watersheds. Some amount of sediment deposition is important for water quality and aquatic habitats, since it provides nutrients and promotes vegetation and habitat growth. However, excess sediment deposition can damage habitats and alter the structure of the waterway. In addition, suspended sediment can cloud the water, preventing sufficient sunlight penetration for aquatic autotrophs (Bilotta & Brazier, 2008). Thus, poor water quality is usually associated with high turbidity and high amounts of total dissolved and suspended solids, which are the results of high sediment transport to a body of water. In this study, the actual impact of fire on the hydrological system will be examined by comparing the amount of total suspended and dissolved solids found in the watershed's bodies of water before and after the fire.

2.2 Assessing Post-Fire Damage to Soils and Hydrology Using GIS-integrated Models

Hydrological modelling is a widely used approach for studying catchment characteristics, roles and behaviors in a hydrological system (Zhou et al. 2013). For example, a hydrological model can estimate runoff, soil erosion or sediment delivery of a catchment. There are many hydrological models used by researchers, each with its own specific parameters, scope, objective and limitations. When investigating the impact of wildfire on hydrological processes, model inputs can include fire temperature and extent, vegetation cover, slope, elevation, soil properties and weather conditions. Outputs depend on the purpose of the model and can include surface runoff, soil erosion rates, or sediment delivery (Aksoy & Kavvas 2005). Assessing post-fire hydrologic responses requires data on the spatial and temporal heterogeneity of the study area. Field-acquired data is often expensive and untimely (Vafeidis et al. 2007). Remote sensing provides an excellent alternative that is more cost-efficient and reliable as it can sometimes be used to monitor both active fires and post-fire conditions (Vafeidis et al. 2007). When integrated into a GIS, remotely sensed data is an essential tool used by researchers, land managers and decision makers to assess the hydrologic responses of an event such as wildfire.

Miller et al (2003) studied the effect of the Cerro Grande fire of 2000, which burned 15,000 hectares, on erosional processes. The RUSLE model was integrated into a GIS program, where pre- and post-fire erosion was estimated. Pre- and post-fire vegetation cover data was derived from Landsat imagery, and the rainfall runoff factor was derived from average annual rainfall amounts. The RUSLE results included an estimated erosion rate range of 0.45 to 9.22 tonnes $\text{ha}^{-1} \text{yr}^{-1}$ before the fire and an estimated erosion rate range of 1.72 to 113.26 tonnes $\text{ha}^{-1} \text{yr}^{-1}$ after the fire. The results suggest that erosion rates increased, on average, after the fire. In addition, when the results were run using fifty-year interval rainfall amounts instead of

average annual rainfall amounts, erosion rate estimations increased by about 3.7 times, suggesting that rainfall amount and intensity following the fire has a great effect on erosion processes.

Mallinis et al. (2016) studied soil loss on the Mediterranean fire-prone island of Thassos, Greece between the years of 1984 and 2013 using remotely sensed data in a GIS. The influence of wildfire-induced land cover changes on hydrological processes was of particular interest. Mallinis et al. used the Revised Universal Soil Loss Equation (RUSLE), noting that it is one of the more widely used models because it is simple and does not have a high data demand. South-facing slopes were found to be the most at risk of land degradation, and risk of soil loss increased the most at higher elevations during the study period. It was found that wildfire yielded increased soil erosion at the catchment level for years following severe fires.

Wilson et al. (2001) used a hillslope elevation model (HEM) within a GIS program to determine the effect that the Cerro Grande fire in New Mexico had on erosion and sediment delivery to streams in which water from the burned catchment would run. Digital flow pathways were created using the model in GIS to determine the deposition, transport, rill and interrill erosion. The HEM model was used because it takes into account nuances in the terrain and their impact on the flow of water in the hydrological system. Model parameters included vegetation cover, slope, soil type and burn severity. A 100-year rain event was run to find the impact in the burned area. It was concluded that the fire may have resulted in a three to six time increase in erosion and a sediment yield increase of more than one magnitude. The model was most sensitive to post-fire vegetation cover and its effect on terrain.

Mallinis et al. (2009) modelled post-fire soil erosion risk in Greece's Kassandra Peninsula for the purpose of prioritizing high risk watersheds for mitigation. A pre-fire ASTER

image, post-fire aerial images and a post-fire Landsat TM image were used to map burn severity, land use and land cover. After mapping burn severity, post-fire sediment yield was estimated with the Erosion Potential Model (EPM) and compared to the pre-fire sediment yield to determine the effect of wildfire on soil erosion in a Mediterranean forested ecosystem. It was found that, while heavy erosion classes prior to the fire covered 55% of the study area, heavy erosion classes covered 90% of the burn area after the fire. The results also concluded that the fire redistributed the spatial pattern of the erosion process in 21 of 24 watersheds, which is noteworthy, as landscape heterogeneity directly affects runoff and soil erosion.

Concerned with the hydrological impact of fires on catchments, Vafeidis et al. (2007) suggests a method of mapping and determining the risk of runoff and soil erosion in four regions of Greece affected by wildfire. GIS and remote sensing were used to estimate model parameters affecting runoff and erosion, including fire temperature and extent, vegetation cover, and slope. Similar to Mallinis et al. (2009), the model was run twice for each region, pre- and post-fire, in order to compare runoff and erosion rates and determine the effect of fire on hydrological processes. The results found that, on average, erosion rates increased 5.7 times after the fire's passage and that slope and vegetation cover had a greater impact on the erosion estimates than did fire extent and temperature. In addition, a change in the spatial distribution of erosion rates was found post-fire.

While many soil erosion models exist, this study used the RUSLE model to estimate soil loss before and after the Pozo fire. The RUSLE model was chosen because it is one of the simplest and widely used models to estimate annual soil loss by water on disturbed slopes. In addition, the data needed to compute the equation is free and available to the public and requires little or no pre-processing.

2.3 RUSLE Model Development

The Universal Soil Loss Equation (USLE) was first developed by the National Resources Conservation Service (NRCS) and published in the U.S. Department of Agriculture (USDA) Agriculture Handbook 282 in 1965 and later updated in the USDA Agriculture Handbook 537 in 1978. It was developed to enable planners to estimate long-term average soil losses from raindrop-impact and surface runoff in response to various combinations of crop systems and management practices, with respect to topography, rainfall events and soil characteristics. In 1992, a computerized version of USLE was developed, resulting in the Revised Universal Soil Loss Equation (RUSLE) (USDA 1997). Today, RUSLE is a widely used soil loss model, and it is commonly integrated in a GIS program, which provides the spatial framework in which RUSLE factors can be derived. The RUSLE model has some limitations. For one, it predicts soil loss best at the hillslope scale, although it can be used at the watershed scale. However, the model is not appropriate at the regional scale. In addition, it predicts only sheet and rill erosion, taking into account soil loss and sediment yield. It does not predict sediment transport or deposition (USDA 1978). For the purpose of this study, the RUSLE model is sufficient, since the scale of the study area is less than the watershed scale. In this study, no attempt at altering or improving the RUSLE model was made. Although it is recognized that the results are simply estimates and not the actual erosion rates, the estimates are useful in risk analysis and mitigation prioritization. The RUSLE model estimates average annual soil loss using the following equation:

$$A = R * K * LS * C * P$$

Where A is the average annual soil loss (tonnes(ha*yr)⁻¹); R is the rainfall erosivity factor (MJ*mm (ha*hr*yr)⁻¹); K is the soil erodibility factor (tonnes*ha*hr(ha*MJ*mm)⁻¹); LS is the

slope length and slope steepness factor; C is the land cover management factor; and P is the conservation practice factor.

2.3.1 Rainfall and Runoff Factor (R)

The rainfall and runoff factor (R) must quantify the effect of raindrop impact and reflect the amount and rate of runoff associated with rain. According to research by the USDA, when other RUSLE factors are held constant, soil loss is directly proportional to the R factor. In general, R factors are considered to be constant for a specified area. Rainfall and runoff factor values for the contiguous United States can be found from erosivity maps derived by the USDA (USDA 1997). When existing erosivity maps do not provide a fine enough scale for a study area, more accurate R values can be calculated using the equation, when rainfall data is available:

$$R = \frac{\sum_{i=1}^j (EI_{30})_i}{N}$$

where E is the total storm energy, I_{30} is the maximum 30-minute intensity, and j is the number of storm events in N number of years. When the total storm energy (E) is multiplied by the maximum 30-minute intensity (I_{30}), the result is the total energy of a rainstorm, called the energy intensity factor. The energy of a storm is a function of the amount of rain and intensity. As the intensity of a storm increases, the raindrop size and velocity also increase, which results in increased kinetic energy that can potentially detach soil particles.

2.3.2 Soil Erodibility Factor (K)

The soil erodibility factor (K) describes the characteristics of the soil and its susceptibility to erosion by rainfall and runoff. Fundamentally, soil erodibility is defined by Renard et al. as the change in soil per unit of applied external force (USDA 1997). Practically,

the soil erodibility factor is a parameter representing the average annual soil and soil-profile reaction to hydrological processes, including but not limited to detachment by raindrop impact, sediment transport by surface runoff, and infiltration into the soil (USDA 1997). K values can be calculated based on the soil-erodibility nomograph, described by the equation:

$$K = [2.1 * 10^{-4}(12-OM) M^{1.14} + 3.25(s-2) + 2.5(p-3)] / 100$$

Where OM is the percent organic matter, M is the product of the percent modified sand and percent modified silt, s is the structure class and p is the permeability class. K values range from 0.02 to 0.69, where smaller K values represent soils that are less susceptible to erosion and larger K values represent soils that are more susceptible to erosion (USDA 1978).

2.3.3 Topographic Factor (LS)

The topographic factor (LS) accounts for the impact of topography on erosional processes. The topographic factor takes into account both the slope length factor (L) and the slope steepness factor (S). In general, as slope length increases, erosion also increases. The slope length is given in the RUSLE model by L, the slope length factor. Linearly, the slope length is the horizontal distance between the origin of surface runoff and the point where either deposition begins to occur or where runoff becomes concentrated into a channel. Two dimensionally, slope length is the upland drainage area per unit of contour length (Miller et al. 2003). With a GIS, the slope length can be more accurately calculated for complex terrain using a DEM. The slope steepness factor (S) takes into account the effect of slope gradient on soil loss when compared to the standard plot with steepness of 9%. As slope length and slope steepness increase, subsequent surface runoff velocity increases allow more soil to be detached. Therefore, slope properties have

a great impact on soil loss. The slope length and slope steepness factor are combined in the RUSLE equation to form the topographic factor (LS), given by the equation:

$$LS = \left(\frac{l}{72.6}\right)^m (65.41 \sin^2 \theta + 4.56 \sin \theta + 0.065)$$

Where l is the slope length, θ is the downhill slope angle (%) and m is a coefficient based on percent slope. The value of m is 0.5 if the percent slope is 5 or more, 0.4 on slopes of 3.5 to 4.5 percent, 0.3 on slopes of 1 to 3 percent, and 0.2 on uniform gradients of less than 1 percent.

2.3.4 Land Cover Management Factor (C)

The land cover management factor (C) accounts for the combined effect of all the cover and management variables. It is the ratio of soil loss from land cropped under specified conditions to the corresponding loss from clean-tilled land. Soil loss from a field continuously in fallow condition is calculated by the product of the R, K and LS factors. However, soil loss from a cropped field is typically less, determined by cover, management practices, land use residuals and crop sequence. Soil loss is also influenced by vegetation cover and growth. Thus, the C factor takes into account these conditions to improve soil loss estimates (USDA 1978).

The cover factor plays an important role in determining soil loss, and it is the factor that changes the most after wildfire. Since the RUSLE model was developed for agricultural purposes, the Agricultural Handbook provided by the USDA does not explicitly explain the methods for determining the C factor for non-agricultural land (forested and urban). A common method for deriving the C factor for non-agricultural land is the use of pre-determined values for certain land use/land cover classes. The Anderson classification method was chosen for this study because it was developed for national use in the U.S. at both the state and federal level (Anderson 1976). Therefore, it is an accepted and common land use classification method.

LULC class values are then spatially represented using existing thematic maps or classified remotely sensed data (Mallinis et al. 2016).

2.3.5 Conservation Practice Factor (P)

The conservation or support practice factor (P) is defined as the ratio of soil loss with a specific support practice to the corresponding loss with up-and-down slope culture (USDA 1978). Contour tillage, strip cropping and terrace systems are considered support practices that are taken into account with the P factor. Practices such as improved tillage practices, sod-based rotations, fertility treatments and crop residues left on the field are erosion control practices exercised by farmers. However, these practices do not affect the P value. Instead, they are taken into account in the C factor as they are considered conservation and management practices. In general, agricultural land use areas are given a P value of 1, as it is assumed that farmers use conservation practices to protect against erosion. Other land use classes are given a P value of 0, since it is assumed that no conservation practice is used on non-agricultural lands.

2.4 Impact of DEM resolution on Spatial Analysis

A digital elevation model (DEM) maps the elevation of an area and can be used for the automation of input parameters for a hydrological model (Prodanović et al. 2009). For example, catchment slopes, subcatchment delineations and flow direction can be represented in a DEM. Surface derivatives such as these can be directly used in model applications such as predictive soil mapping (Thompson et al. 2001), hydrological models (Vafeidis et al. 2007; Zhou et al. 2013), and erosion models (Wilson et al. 2001; Aksoy & Kavvas 2005). Because model inputs are often derived from the DEM, ensuring accuracy of the DEM's source data is crucial in

obtaining successful model results. (Buakhao & Kangrang 2016). Error involved in topographic analysis may stem from inaccuracies in source data, DEM interpolation methods or from the algorithm chosen (Wise 2000; Claessens et al. 2005).

Grid DEMs are the most widely used DEM type (as opposed to a triangulated irregular network) since they are the simplest form and they are compatible with other data types used in a GIS (Gao 1998; Claessens et al. 2005). Because of the way data is stored, grid DEMs innately have limitations. An important aspect involved in the use of grid DEMs for hydrologic modelling is that of DEM resolution, or grid size. A grid DEM attempts to represent real-world continuous surfaces and contours as grid cells, where only one elevation value can be assigned to each pixel and where surface derivatives are simply estimations. Therefore, the size of the cells sets constraints and affects the precision of a dataset. (Claessens et al. 2005). DEM resolution impacts the level of accuracy and detail available for input data and the time and cost necessary to compute the model outputs (Prodanović et al. 2009). High resolution DEMs require more time to run models than low resolution DEMs and can sometimes contain unnecessary information that will complicate the results (Passalacqua et al. 2015). When time or budget is a limiting factor, coarser DEMs may be used to reduce computation time. However, coarse DEMs can fail to detect hydrologic or geomorphic heterogeneity, resulting in underestimated model outputs (Thompson et al. 2001; Lisenby & Fryirs 2017). Thus, choosing DEM resolution is a decision a researcher must make before model computation, based on the scale and scope of the study area, research objective and model complexity (Lisenby & Fryirs 2017). Selecting the appropriate DEM resolution for hydrologic analysis is not simple, and the implications of DEM resolution on model analysis are being explored by researchers.

Mitra et al. (1998) determined the effect of resolution of input data on fuzzy logic model outputs and compared the soil erosion predictions of fuzzy logic methodologies with those of the Universal Soil Loss Equation (USLE) at the watershed level. Coarser resolution data resulted in decreased predictions of high soil erosion areas. Soil erosion areal extent and erosion class distribution results from the USLE model and the two-variable-fuzzy logic model were similar, whereas the USLE model and the three-variable-fuzzy logic model results differed mostly in moderately low and moderate erosion classes, probably because of the rainfall erosivity and conservation practice variables used in the USLE model and excluded in the fuzzy logic model. Overall, fuzzy logic models were shown to be an easy, low-input methodology for predicting soil erosion potential at the watershed level and suggested that coarse resolution data is better suited for regional scales because it is most cost-effective, but finer resolution data is better for local areas at larger scales.

Schoorl et al. (2009) quantified the effect of spatial resolution on modelling the processes of erosion and sedimentation. The only factors that were manipulated were DEM resolution and the method of flow routing. Contrary to expectations, soil loss prediction increased as spatial resolution increased with all flow routing methods. An increase in soil erosion predictions of 97.5% occurred between the finest resolution (1 m) and the coarsest resolution (81 m), meaning soil loss estimates almost doubled.

Buakhao and Kangrang (2016) conducted a SWAT model analysis using three DEM resolutions (5m, 30m, and 90m) on both flat and mountainous terrains and on three catchment areas (20,000, 200,000, and 1,500,000 hectares) to determine the impact of DEM resolution on analysis results for varying study area types and sizes. The results demonstrated that DEM resolution had a significant impact on catchment area slopes, but not on catchment size and

shape and that the greatest differences were found in large catchment areas compared to small catchment areas. It was concluded that DEM resolution impacts watershed delineation and stream network but that there is no significant advantage to using a finer resolution. Instead, the results showed that a coarser resolution saves time and is sufficient for hydrologic modelling.

Tan et al. (2015) compared the results of a SWAT model estimating streamflow of the Johor River Basin of Malaysia when using varying DEM resolutions (20m to 1500 m), DEM sources and resampling techniques. Compared to DEM source and resampling technique, DEM resolution had the greatest impact on SWAT model results for streamflow simulation. DEM resolution had a smaller impact in larger catchments and greater impact in smaller catchment. It was found that finer resolutions did not yield greater accuracy in streamflow predictions. Resolutions resulting in the most accurate streamflow predictions were those between 20m to 50m and 100m to 800m.

For the purpose of this study, DEM resolution is important for the computation of the topographic factor used in the RUSLE model. The topographic factor consists of slope steepness and slope length, which are derived from a digital elevation model of the study area. Therefore, the resolution of the DEM used to determine the slope steepness and length has an influence on the results of the RUSLE model because DEMs of differing resolutions will exhibit varying landscape profiles. Since slope plays an important role in the erosion process, soil erosion modelers would benefit from understanding the effects of DEM resolution on RUSLE outputs in order to yield the most accurate soil loss estimates. Choosing the DEM resolution to use for the model is not simple or concrete because the implications of DEM resolution have varying impacts. For example, some studies have found that lower DEM resolutions may underestimate soil loss because larger grids may result in loss of data and high errors, and they suggest that

finer resolutions yield more accurate results (Gallant 2001; Zhang et al. 2008). However, very fine resolutions (<10m) may contain unnecessary information that can complicate the results, possibly overestimating soil loss in erosion modelling. In addition, higher resolution data is not available for all study areas, in which case coarser resolution data must be used. Therefore, there is a trade-off necessary in order to maximize result accuracy with the available data for each study area. This study will determine the impact of DEM resolution on RUSLE results so as to provide information that may aid researchers and modelers in choosing the appropriate data resolution for erosion modelling.

3 Study Area

The Pozo fire occurred in Los Padres National Forest (Main Division), located in San Luis Obispo County, California, and burned an estimated 466 hectares (Figures 1 and 2b). The fire started on August 21, 2010 and was contained by August 22, 2010. The cause of the fire is unknown. The fire was located near Pozo Road, southeast of the Santa Margarita Lake. It was a vegetation fire on federal land, and several nearby campgrounds and roads were evacuated (California Department of Forestry and Fire Protection 2010). One thousand personnel were assigned to the fire and the suppression costs totaled \$1.5 million (Santa Maria Times 2010). See Appendix A for a severity map of the Pozo fire.

The Pozo fire took place near the river head of the Salinas River, a major river in the Salinas watershed that empties into Monterey Bay (Figure 2a). The topographic map displayed in Figure 3 demonstrates that the Salinas River flows northward toward the Monterey Bay due to the topography of the area, including the widening valley and floodplain as the river approaches the bay. Figure 4 indicates the streamflow of the Salinas River when overlaid on the DEMs for

Salinas watershed. These maps justify the rainfall, discharge and water quality stations used, as they are located downstream of the fire.

The climate of Pozo, California, located near the west coast of southern California, is warm- to hot-summer Mediterranean. Summers are warm and dry with little to no rain, while winters are mild but chilly. Moderate precipitation occurs in the colder months. The mean annual precipitation in Los Padres National Forest's Main Division ranges from 250 mm to 1000 mm (Moritz 1997; Daly et al. 1994), with the mean annual precipitation of San Luis Obispo County for 1981-2010 being 587mm (National Oceanic and Atmospheric Administration). In the December and January following the Pozo fire, however, the Salinas watershed experienced 371 mm of rain- a considerable portion of the mean annual precipitation for the area. The mean annual temperature for San Luis Obispo County is 15.0°C, with mean maximum July temperature 18.1 °C and mean minimum January temperature 11.4°C (NOAA). Elevation of the burn area ranges from 486 m to 844 m. The predominant vegetation making up the forest is chaparral and coastal sage scrub. Both vegetation types have evolved certain fire adaptations, often having maximum reproductive success in post-fire conditions (Moritz 1997).

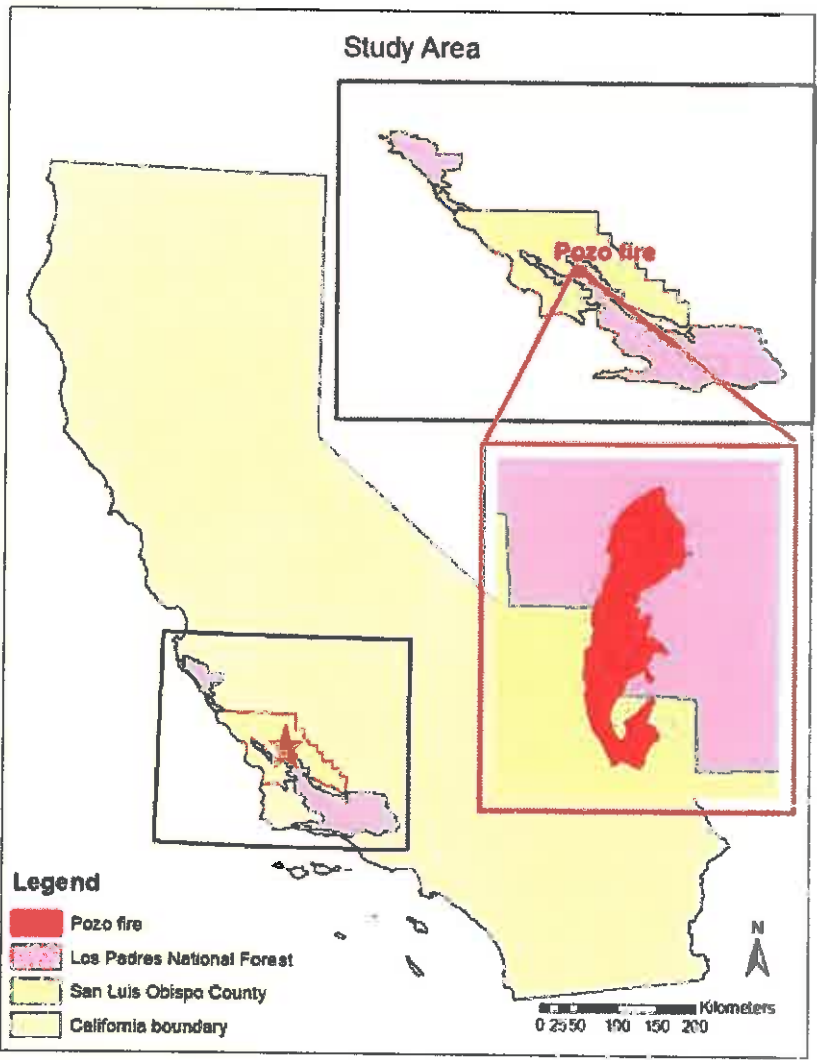
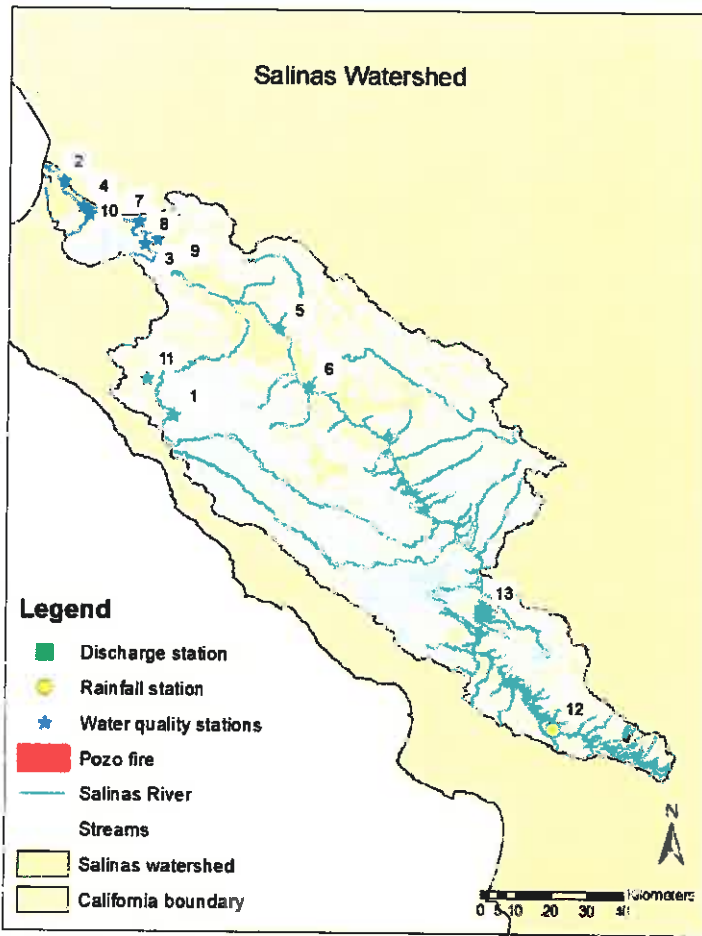


Figure 1. Study area overview

2 a)



Alias	Type	Station Location	Station ID
*1	Water quality	Arroyo Seco	*309ARSARC
2	Water quality	Blanco Drain	309BLA
3	Water quality	Chualar Creek	309CRR
4	Water quality	Salinas River	309DAV
5	Water quality	Salinas River	309GRN
*6	Water quality	Salinas River	*309PS0072
7	Water quality	Quail Creek	309QUI
8	Water quality	Salinas River	309SAC
9	Water quality	Salinas River	309SAG
10	Water quality	Salinas River	309SSP
*11	Water quality	Willow Creek	*309WLCATC
12	Rainfall	Salinas Dam	USC00047672
13	Discharge	Paso Robles	11147500

Figure 2 a) Salinas watershed including major rivers and streams, Pozo perimeter and rainfall/water parameter station locations

2 b)

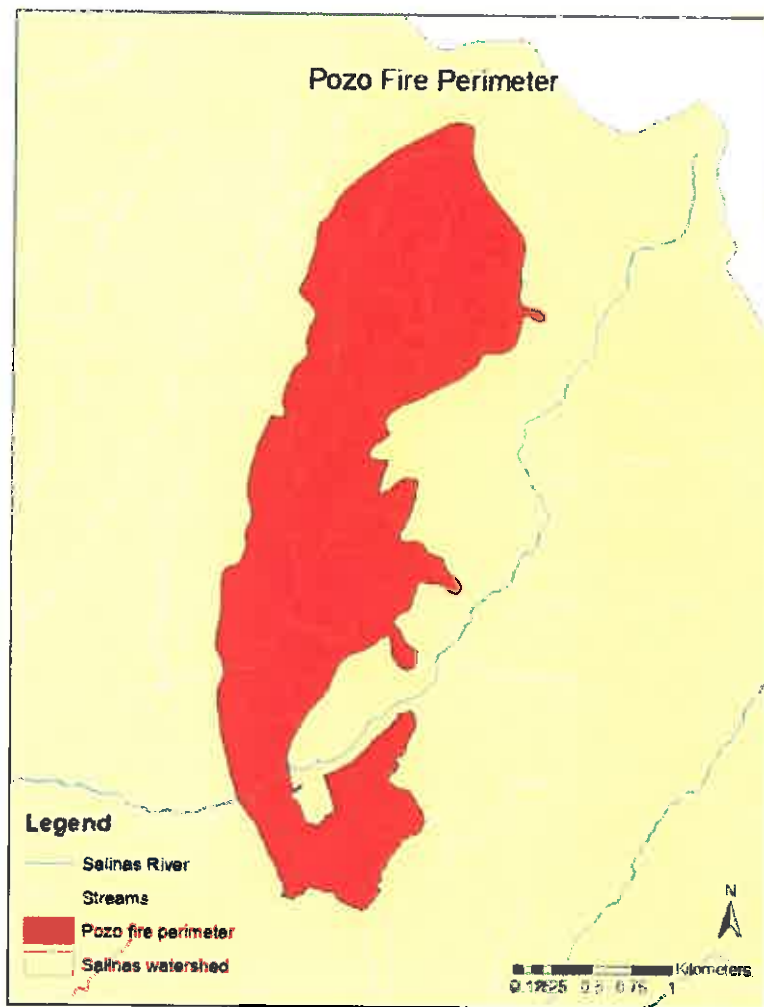


Figure 2 b) Pozo fire perimeter close up



Figure 3. Topographic map of California

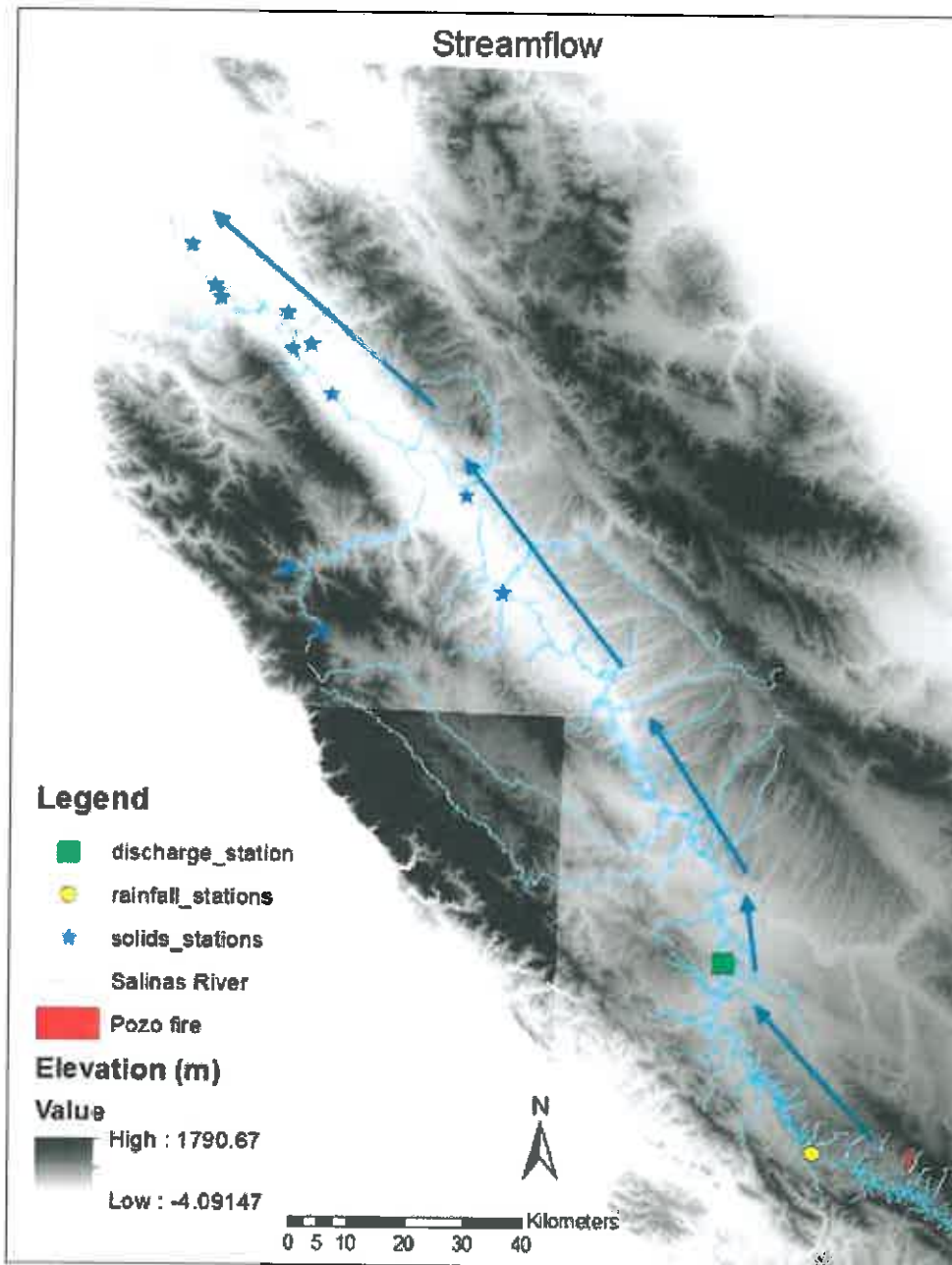


Figure 4. Streamflow map with arrows indicating streamflow direction

4 Methodologies

In this study, the RUSLE model was used to estimate soil loss rates before and after the 2010 Pozo fire. The RUSLE model was chosen because of its simplicity, the availability of data, its empirical framework, its compatibility within a GIS format and its wide use. Spatial inputs for

the RUSLE factors were derived from existing geospatial databases and were integrated within a GIS program (ArcMap), where the RUSLE model was run. Of the inputs used in the RUSLE model, land/vegetation cover varies the most before and after the fire, while the other inputs are considered constants. This makes for a relatively easy and efficient method of comparing pre- and post-fire soil erosion rates to determine the impact of wildfire on the hydrological system.

The RUSLE model was run again using various DEM resolutions for the LS factor to determine the effect of DEM resolution on RUSLE results. DEM resolutions of 30m and 90m were used to derive the LS factor, and the RUSLE equation was run under each condition, using the landcover data (C factor layer) for before the fire (year 2006). Then the results of both the 30m and 90m RUSLE runs were compared to determine the impact of DEM resolution on model results.

Finally, since the RUSLE model provides only estimates of soil erosion rates and thus only estimates of the hydrological impact of the Pozo wildfire, actual water quality data from directly before and after the fire was used to determine the actual impact of wildfire on the Salinas watershed.

4.1 Data layer sources and processing

The data used for inputs in the RUSLE model were obtained from several agencies and were compiled in a GIS. Table 2 lists the sources of data for each RUSLE layer and for the weather/water quality stations. Section 4.2 describes the manipulations of data and methods used to run the final RUSLE equation.

Table 2. Data layer sources

GIS layer	Source
Pozo Fire Perimeter	CA FIRE FRAP
R factor	USDA
K factor	NRCS SSURGO
LS factor – 30m	USGS
LS factor – 90m	SRTM
C factor	NLCD
P factor	NLCD
Weather/water quality data	Source
Rainfall data	NOAA
Discharge data	USGS
Water quality data	EPA STORET

All data layers were projected to North America UTM Zone 10N in ArcMap. First, fire history data was downloaded from the CA FIRE FRAP database and the Pozo fire perimeter was selected using Select by Attribute. After only the Pozo fire perimeter was selected, the Export Selected Features tool was used to create the study area. Since the study area was in vector format, the shapefile was converted to raster format with 30m grid resolution. All RUSLE data layers were converted to raster (30m) if originally in vector format and then extracted by mask to the Pozo fire perimeter raster file. For the DEM resolution analysis, RUSLE layers were simply resampled to 90m, with the exception of the LS factor, which was calculated using a 90m SRTM DEM. The following figures (Figures 5-9) are the raw input maps used to derive the five RUSLE factors.

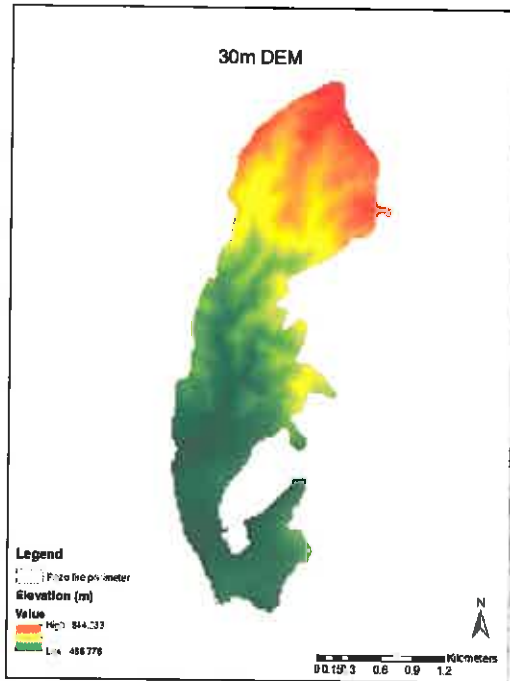


Figure 5. 30m DEM (USGS)

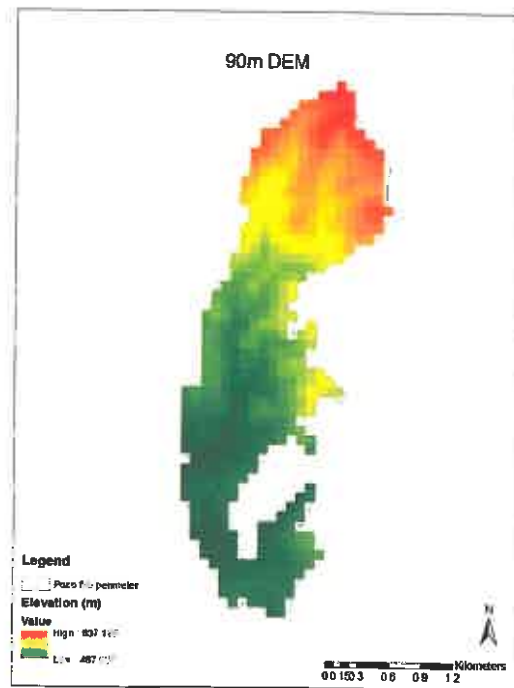


Figure 6. 90m DEM (SRTM)

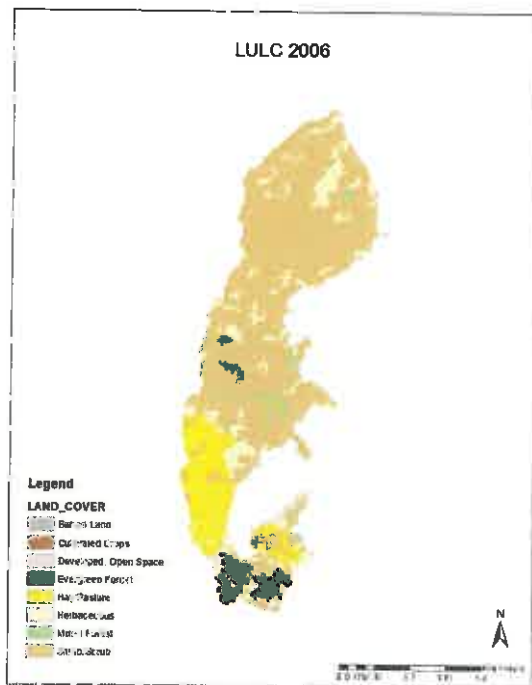


Figure 7. LULC data 2006 (NLCD)

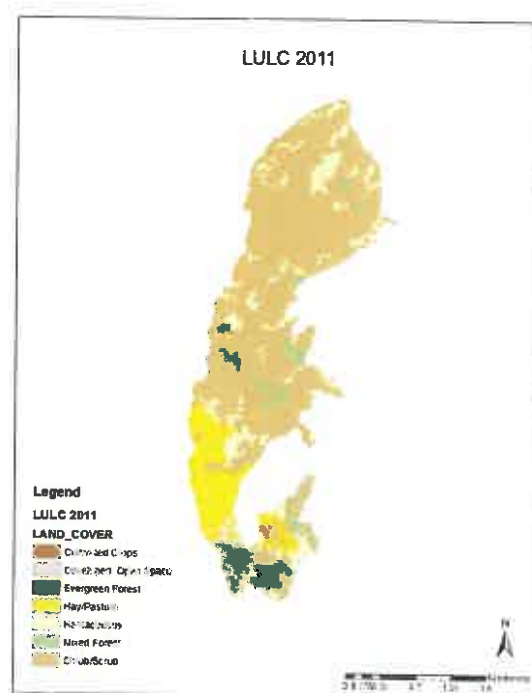
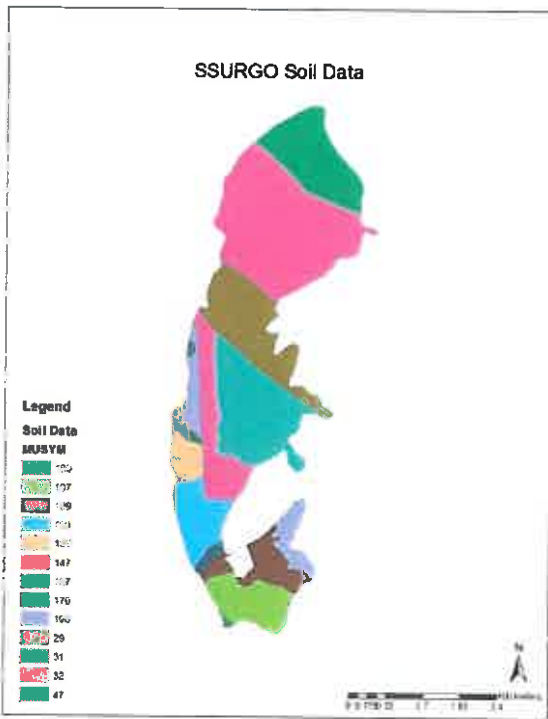


Figure 8. LULC data 2011 (NLCD)



MUSYM	Soil name
100	Arbuckle
107	Arnold
109	Ayar
110	Ayar
135	Dibble
147	Hanford
167	Metz
170	Milsholm
190	Rock outcrop
29	Stonyford
31	Modesto
32	Agua Dulce
47	Trigo

Figure 9. Soils data (SSURGO)

4.2 RUSLE Layers

4.2.1 Rainfall and Runoff Factor (*R*)

While the *R* factor can be calculated using the methods described in section 2.3.1, *R* factors for the contiguous U.S. have already been calculated by the USDA. Isoerodent maps found in the USDA Agriculture Handbook No. 703 were created using 22-year station rainfall data. Isoerodents were located using rainfall intensity/frequency data and topographic maps (USDA 1978). For the purpose of this study, the *R* factor was obtained from the isoerodent map provided in the USDA Agriculture Handbook No. 703 (USDA 1997). The units of the *R* values on the map (Figure 10) are in U.S. customary units, while the units desired for this study are SI units. Thus, the *R* value for the location of the Pozo fire

(60 hundreds of ft-tonf*in (acre*hr*yr)⁻¹) was multiplied by 17 to convert to SI units, resulting in an *R* value of 1,021 MJ*mm (ha*hr*yr)⁻¹ (Foster et al. 1981). The Pozo fire perimeter raster file

was reclassified to create the R factor layer. All values were reclassified to 1,021, and the output was the R factor layer used in the final RUSLE calculation.

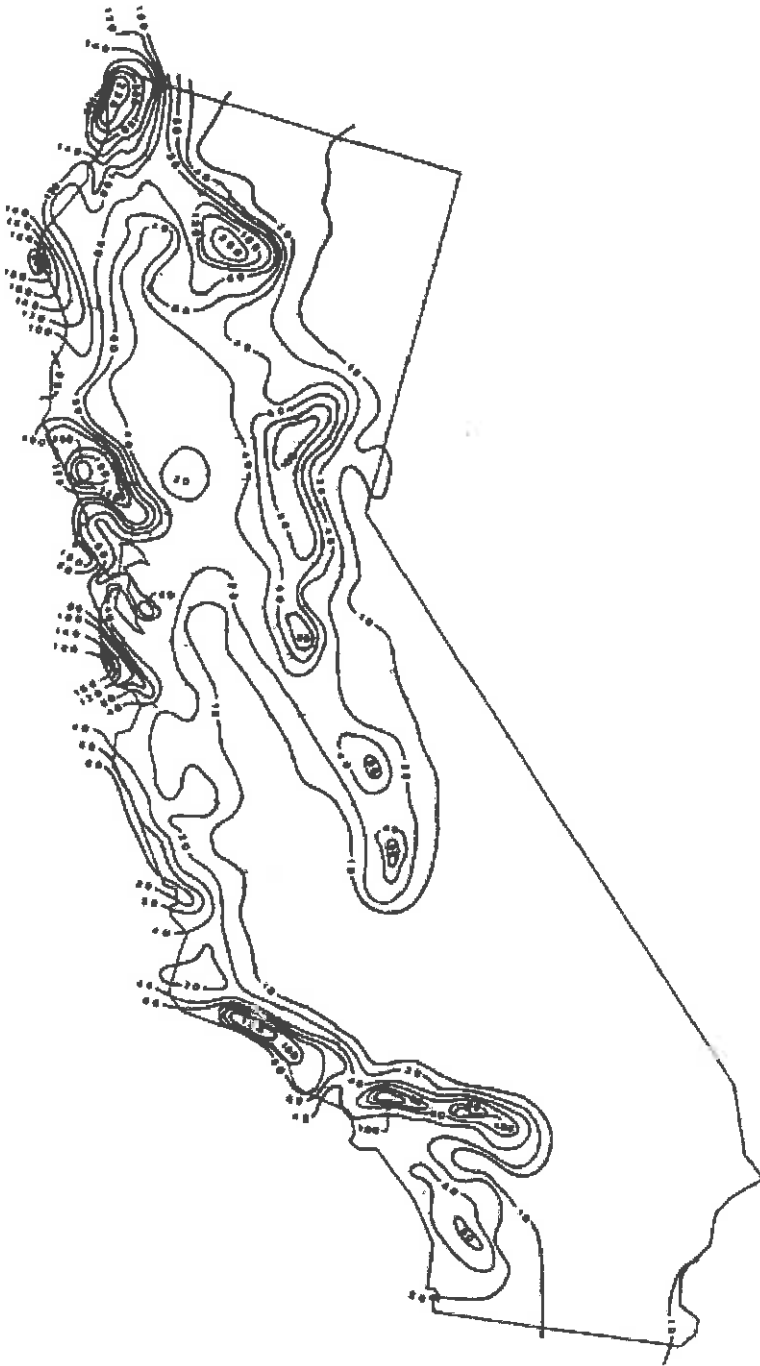


Figure 10. Isoerodent map of California with local R values (USDA 1997).

4.2.2 Soil Erodibility Factor (K)

In this study, K factors were obtained for the study area by downloading soil survey data from the NRCS Soil Survey Geographic Database (SSURGO). From the database, reports with RUSLE related attributes for the study area were exported as tabular data, and spatial soil data was downloaded. In ArcMap, K values were spatially displayed by joining the soil layer to the tabular component data based on the map unit key and by joining the C horizon table based on the component name. This displayed the K values for each soil component type in the attribute table. The K values were float values less than one. In order to do the vector to raster conversion, float values were converted to integer values using the Field Calculator: $K_fact * 100$. Then, the soil layer was reprojected to UTM Zone 10N and converted to raster using Feature to Raster tool based on the K_fact field. The output raster was extracted by mask to the study area. The raster with K values (integers) was divided by 100 using the Raster Calculator.

The units of the K values provided in the SSURGO database were in U.S. customary units ($\text{ton} \cdot \text{acre} \cdot \text{hr} (\text{hundreds of acre} \cdot \text{ft} \cdot \text{tonf} \cdot \text{in})^{-1}$). Thus, the K value raster was converted to SI units ($\text{ton} \cdot \text{ha} \cdot \text{hr} (\text{ha} \cdot \text{MJ} \cdot \text{mm})^{-1}$) using the Raster Calculator. The original cell values were multiplied by 0.1317 to convert to SI units (Foster et al. 1981).

4.2.3 Topographic Factor (LS)

Topographic factor for the study area was derived in ArcMap using the DEM, which was acquired from USGS. First, the DEM was reprojected to UTM Zone 10N and extracted by mask to the study area. The slope map was created using the Slope tool, found in the Spatial Analyst Tools (Surface), and the DEM as the input. The flow direction raster was created using the Flow Direction tool, found in Spatial Analyst Tools (Hydrology), and the DEM as the input. The flow

accumulation raster was created using the Flow Accumulation tool, found in Spatial Analyst Tools (Hydrology), using the flow direction raster as the input. Finally, the topographic factor was calculated using the Raster Calculator in Spatial Analyst Tools (Map Algebra) and the following equation:

$$\text{Power}(\text{"FlowAccumulation"} * \text{Resolution} / 22.1, 0.4) * \text{Power}(\text{Sin}(\text{"Slope"} * 0.01745) / 0.09, 1.4) * 1.4$$

The output raster was the topographic (LS) factor layer for use in the final RUSLE equation.

4.2.4 Land Cover Management Factor (C)

Land cover data for 2006 and 2011 was obtained from the National Land Cover Database (NLCD). The NLCD provides only national land cover data for 2001, 2006 and 2011. Since yearly land cover data was not available for the state of California through NLCD or other free online databases, NLCD land cover data for 2006 was used for the C factor before the fire which occurred in 2010, and NLCD land cover data for 2011 was used for the C factor after the fire. Once the land cover data raster for each year was downloaded, the maps were reprojected to UTM Zone 10N. The Extract by Mask tool in ArcMap was used to clip the map to contain only the study area. The original raster dataset contained Level II landuse classification associated with each cell value. Using this information and Table 3, C factor weights were assigned to the appropriate cell values using the Reclassify tool in ArcMap. The classification method in Table 3 was obtained from the Anderson Classification System (Anderson 1976). The output raster with the appropriate C factor weights was used as the C factor layer in the final RUSLE computation.

Table 3. C factor weights

Landuse Class	Level I Classification (NLCD)	Level II Classification (NLCD)	C Factor Weight
Urban	1	11-17	0.001
Agriculture	2	21-24	0.40
Upland Non-Forested or Rangeland	3	31-33	0.01
Upland Forested	4	41-43	0.003
Water	5	51-54	0
Wetlands	6	61-62	0.0001
Barren	7	71-77	1
Tundra	8	81-85	0.001

4.2.5 Conservation Practice Factor (P)

In this study, it was assumed that all agricultural land uses implement a conservation practice, while all the other land uses do not implement a conservation practice. The land use data layer was used to create the P factor layer. The original NLCD land use raster was clipped to the study area using Extract by Mask tool in ArcMap. Then the Reclassify tool was used to give all agricultural land use cells a P value of 1 and all other land use cells a value of 0. The output raster was the P factor layer used in the final RUSLE computation.

4.2.6 Final RUSLE Equation

Once all five RUSLE factors were created as layers in ArcMap, the final equation was run. Using the Raster Calculator tool, the RUSLE equation was inputted by multiplying each of the five layers. The output was a RUSLE map. The symbology was adjusted to Classified with a Green through Red color ramp to clearly distinguish patterns of varying soil erosion rate estimates. The values were classified into five classes under the Symbology tab (Properties). Table 4 lists the five classes, their parameters and their respective erosion risk potential labels.

In order to use the Tabulate Area tool, it was necessary to reclassify the floating-point file as an integer file using the Reclassify tool. Then the Tabulate Area tool was used to create an area coverage table of each of the five RUSLE erosion class (Millward & Mersey 1999).

Table 4. RUSLE erosion classes

Erosion Class	Soil Loss (tonnes ha ⁻¹ yr ⁻¹)	Erosion Risk Potential
1	< 5	Low
2	5 - 10	Moderately Low
3	10 - 50	Moderate
4	50 - 100	Moderately High
5	> 100	High

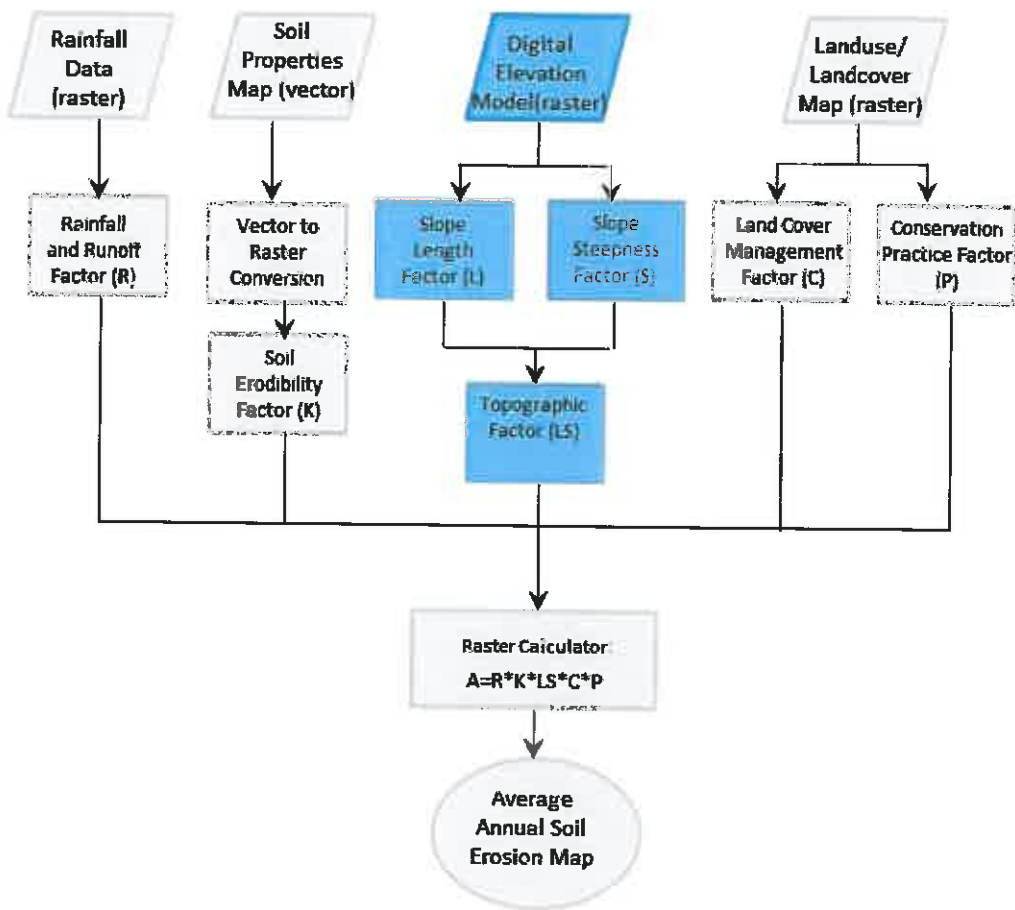


Figure 11. RUSLE model flow diagram

4.3 Assessing Water Quality

Since the RUSLE model provides only estimates of soil erosion rates and thus only estimates of the hydrological impact of the Pozo wildfire, actual water quality data from before and after the fire was used to determine the actual impact of wildfire on the Salinas watershed. As mentioned previously, total dissolved solids (TDS) and total suspended solids (TSS) are indicators of soil erosion and decreased water quality. Water quality (TDS and TSS) data was queried by the Salinas watershed and by the study period (December 2009 to February 2011) on the Environmental Protection Agency's (EPA) STORET Central Warehouse. The data obtained from this query included data from eleven sites located along the Salinas River. See Figure 2a and accompanying table for the location and list of these eleven stations. The stations closest to the fire were of greater interest because they should be more indicative of fire effects on sediment transport to the Salinas River. However, the three closest stations that appear on Figure 2a (station aliases 1, 6, and 11) contained only one data entry each for the study period, and they were for several months *before* the fire. Since the focus here is on the water quality *after* the fire, these three data points were excluded from the analyses in Figures 22 and 24 below. Therefore, station alias 5 was used as the closest water quality station (highlighted black in Figure 22).

These sites were selected because they are downstream of the fire (Figure 4). Therefore, the water quality at these locations can be indicative of the effects of the Pozo fire on downstream aquatic systems. Soil erosion is dependent on precipitation amount and intensity. During droughts or dry seasons, little soil erosion is expected. Since southern California experiences little to no rain during the summer season, water quality data from the rainiest months (December and January) was used to compare TDS and TSS the year before and after the fire in Figure 21.

In addition, monthly rainfall and discharge data for December 2009 to February 2011 were collected from NOAA and USGS stations, respectively. These data were used to determine the amount of precipitation experienced after the fire, and its effect on streamflow, since precipitation drives erosion by water.

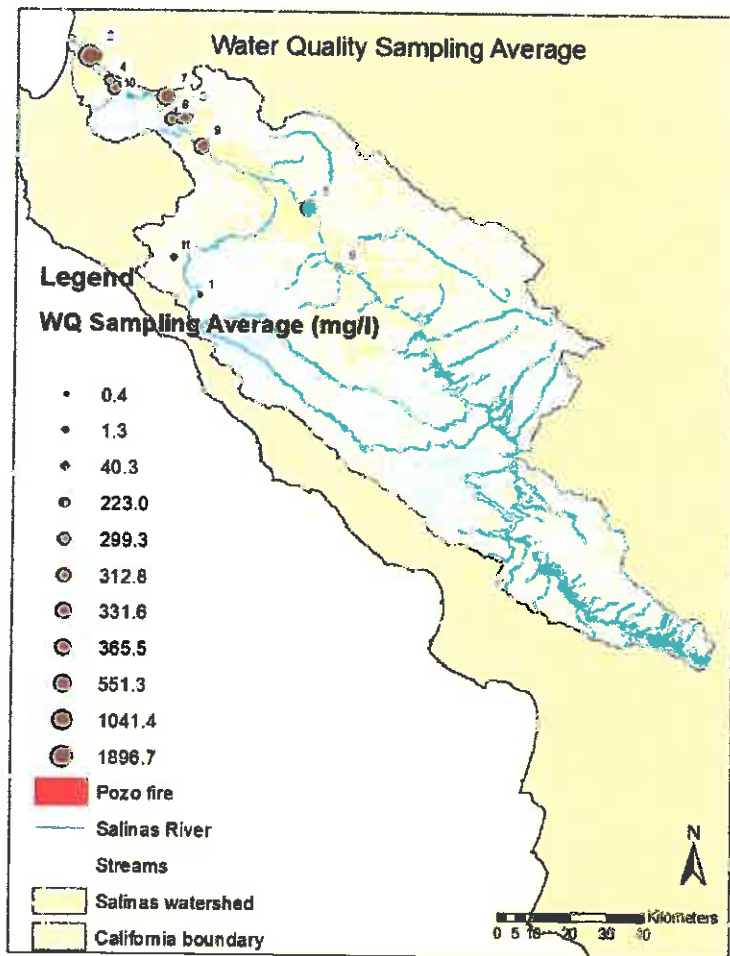


Figure 12. Water quality station sampling average over study time period (December 2009 to February 2011)

4.4 Assessing DEM Resolution Impact on RUSLE Results

This study is also interested in the effect of DEM resolution on RUSLE results. Since the DEM resolution affects the topographic (LS) factor calculation, an LS raster was created for each DEM resolution (30m and 90m) using the methods described in section 4.2.3. The four other

RUSLE layers (pre- and post-fire) were resampled to 90m from 30m for the 90m model so that the cells would align, and the RUSLE equation could be run. Once a RUSLE map for both the 30m and 90m model was produced and values were classified by erosion risk potential (Table 4), percentage area of respective erosion classes were compared to determine the impact of resolution on model results.

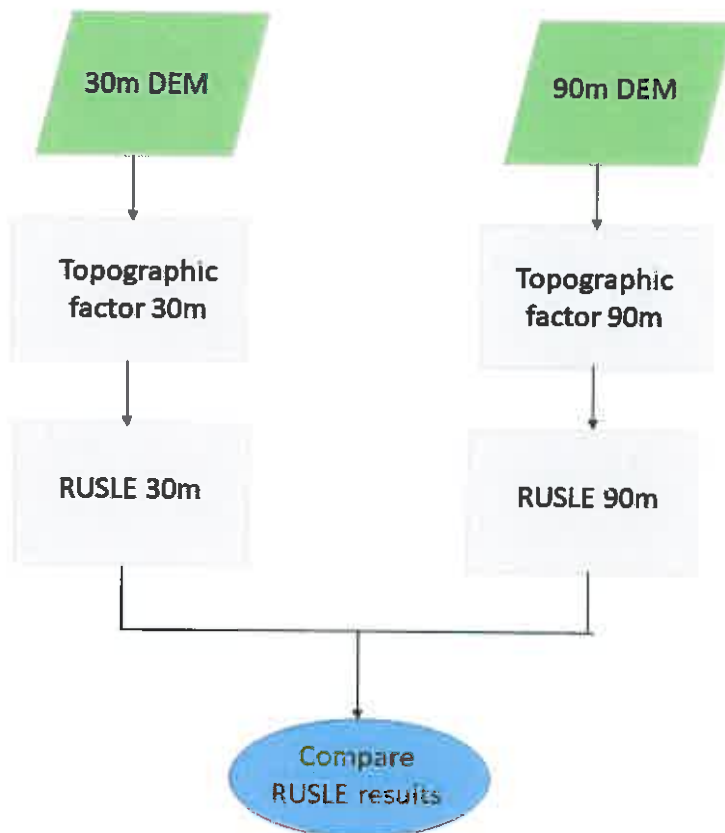


Figure 13. DEM resolution comparison flow diagram

5 Results

5.1 Impact of Wildfire on Soil Erosion

The constant inputs included the rainfall runoff, soil erodibility and topographic factors, which accounted for the geomorphological and climate related parameters. Figure 14 illustrates the constant inputs used for the RUSLE model. The variable inputs included the land cover management and conservation practice factors. Figure 15 illustrates the variable inputs used for the RUSLE model for both the pre-fire and post-fire maps.

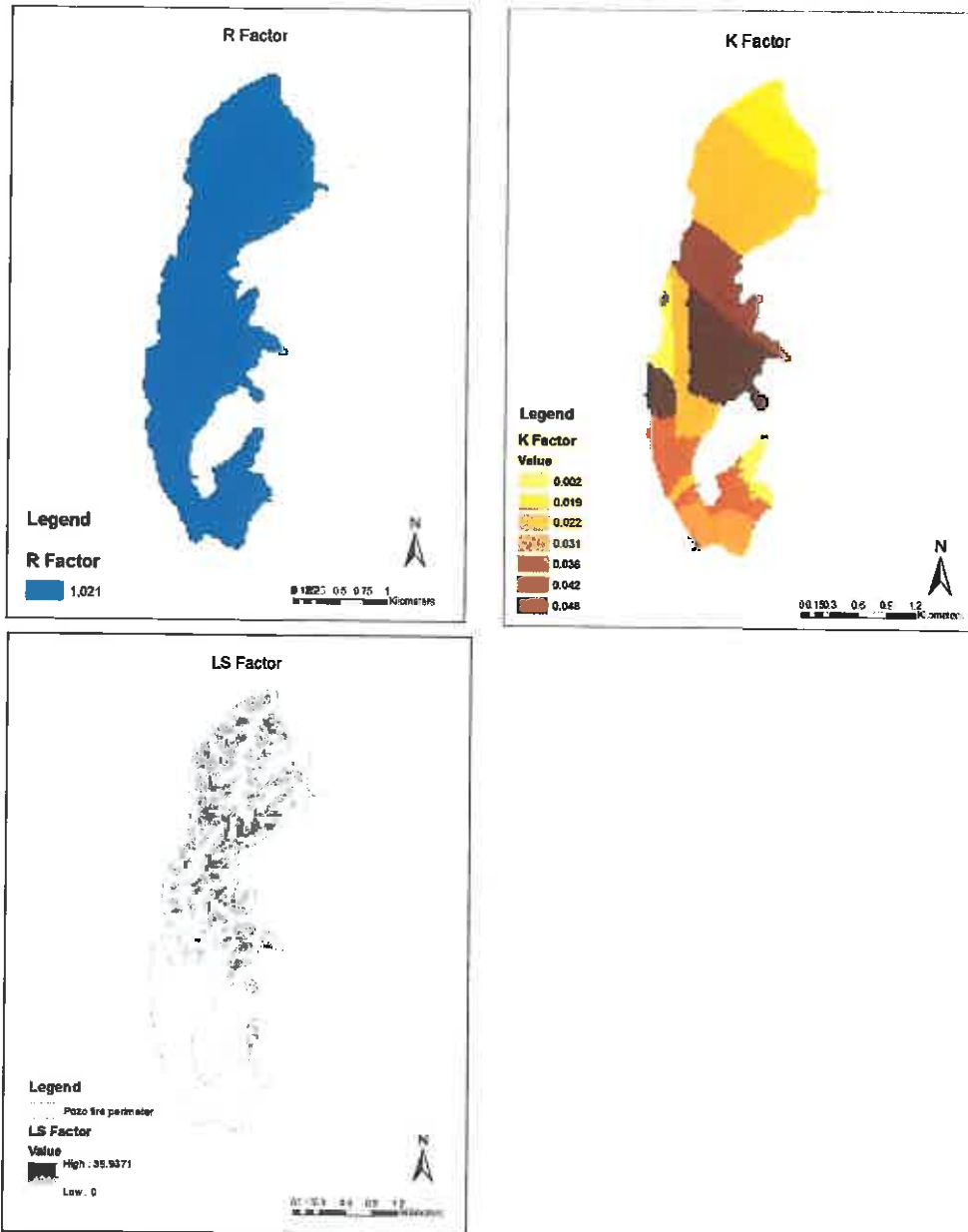


Figure 14. Constant inputs: Rainfall runoff, soil erodibility and topographic factors

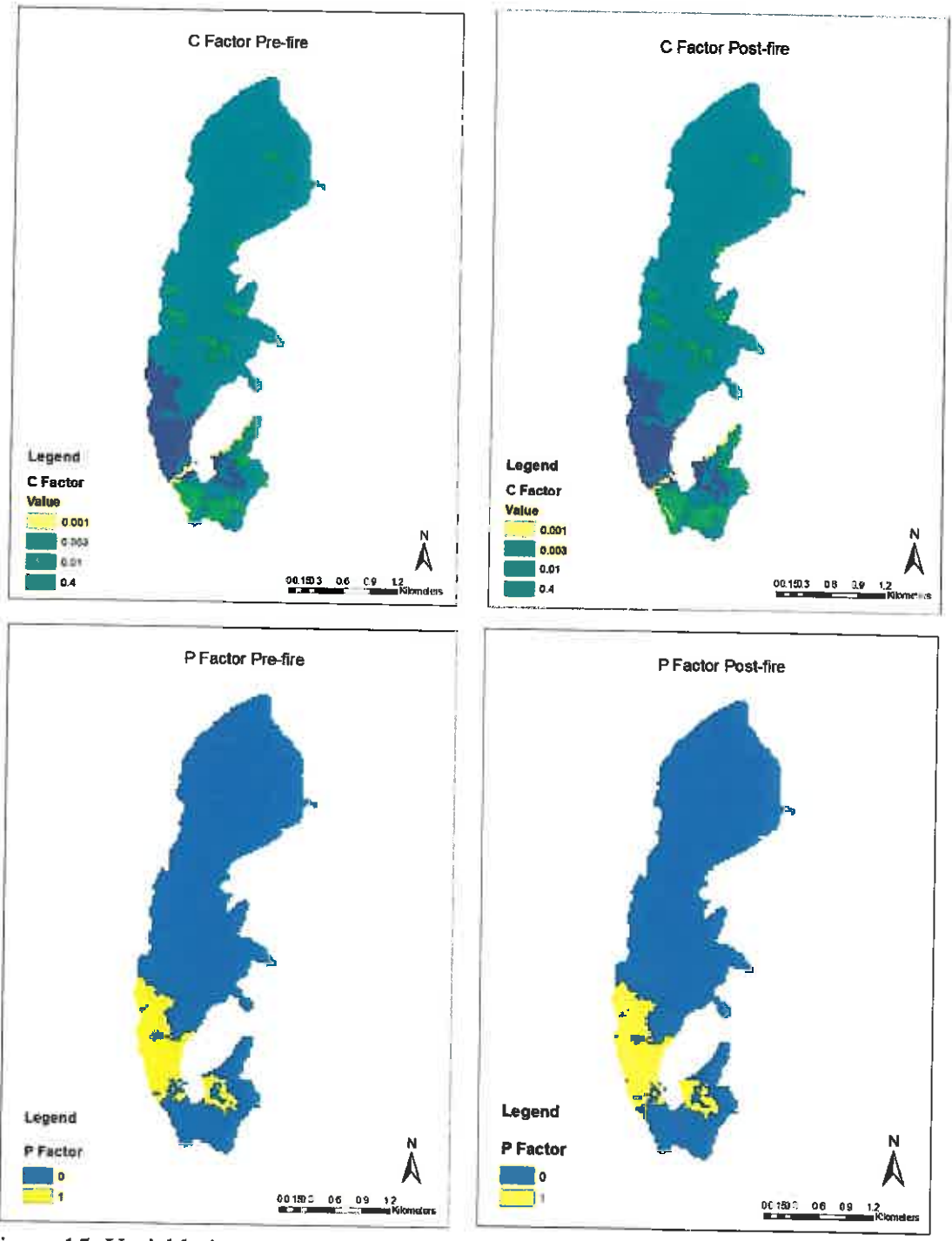


Figure 15. Variable inputs: Land cover management and conservation practice factors

The pre- and post-fire RUSLE maps both yielded results with the majority of the study area (92.0-92.7%) in the first erosion class (low soil erosion risk potential), with only a 0.8%

difference. The second erosion class covered 0.08% of the study area for both the pre-fire and the post-fire, resulting in zero percent difference. The percent area of the third erosion (moderate risk) class was greater by 17.6% after the fire. Area coverage of soil erosion hot spots (moderately high to high risk) increased from 5.5% to 5.9%. The third, fourth and fifth erosion classes increased in area after the Pozo wildfire. Table 5 lists the percent area and area (ha) of each erosion class before and after the fire. However, the value of the maximum soil loss rate was the same for pre- and post-fire RUSLE models. Both conditions resulted in a maximum soil loss value of 341.6 tonnes per hectare per year.

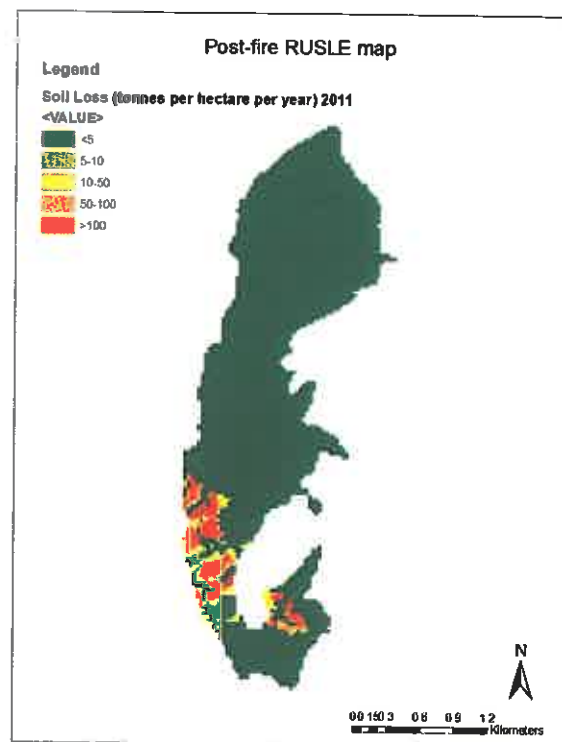
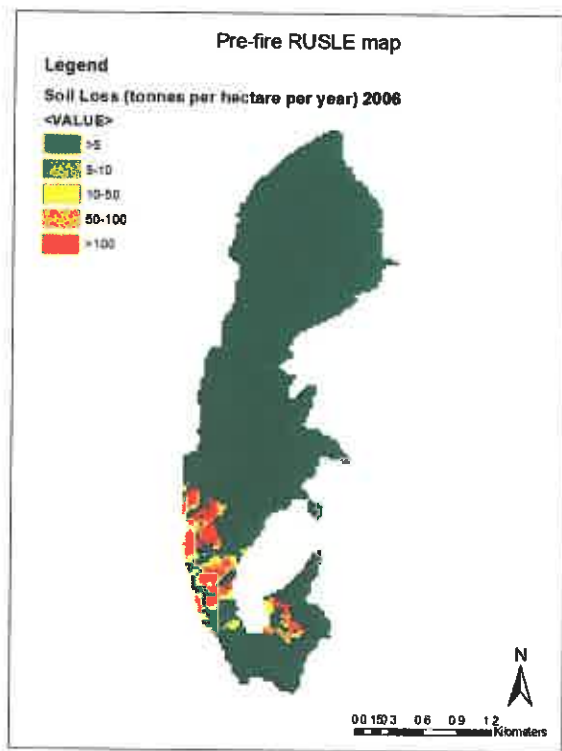


Figure 16. Classified pre-fire soil erosion map Figure 17. Classified post-fire soil erosion map

Table. 5. Comparison of erosion risk classes areal extent between pre- and post-fire (30m)

Pre-fire		
Erosion Risk	Percent Area	Area (ha)
Low	92.7%	432.0
Moderately Low	0.1%	0.5
Moderate	1.7%	7.9
Moderatly High	2.7%	12.6
High	2.8%	13.0
Post-fire		
Erosion Risk	Percent Area	Area (ha)
Low	92.0%	428.7
Moderately Low	0.1%	0.5
Moderate	2.0%	9.3
Moderatly High	2.8%	13.0
High	3.1%	14.4

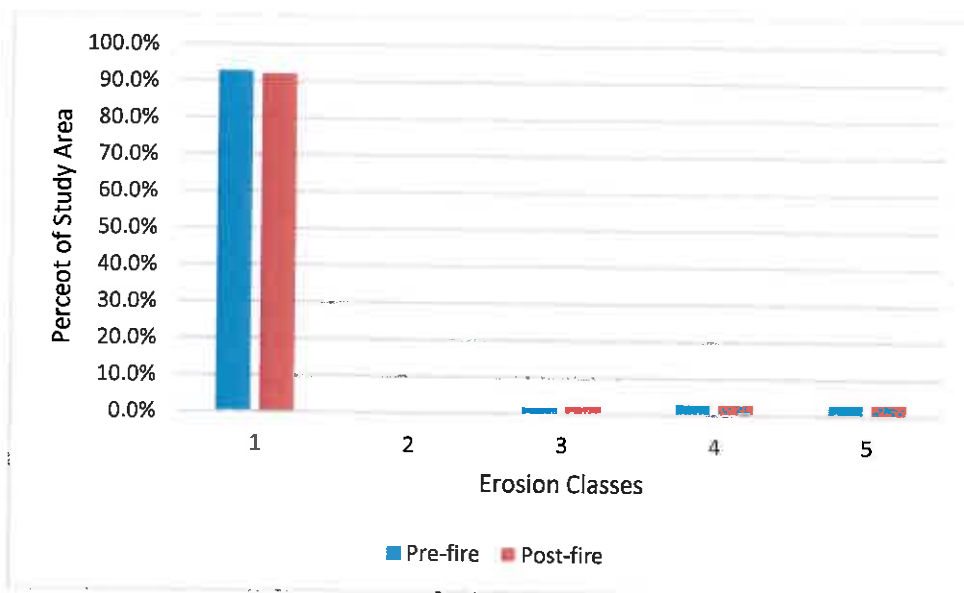


Figure 18. Comparison of erosion class percent area before and after the wildfire (30m)

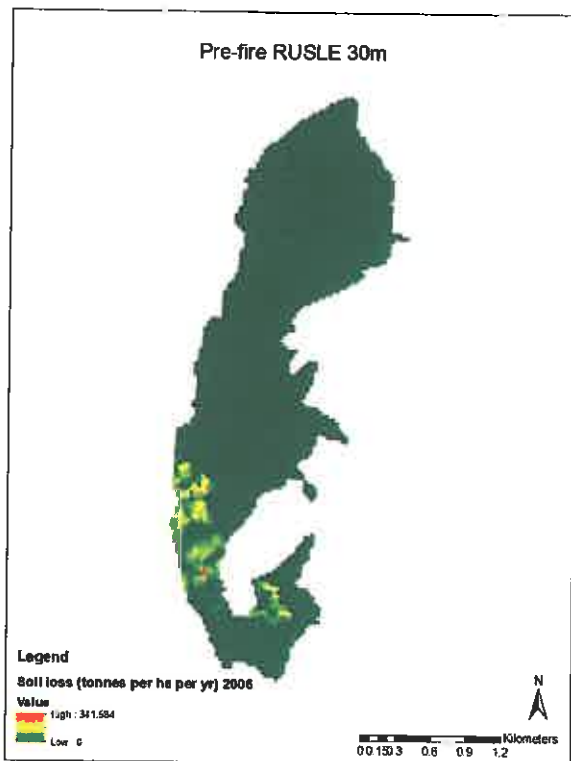


Figure 19. Unclassified pre-fire soil loss

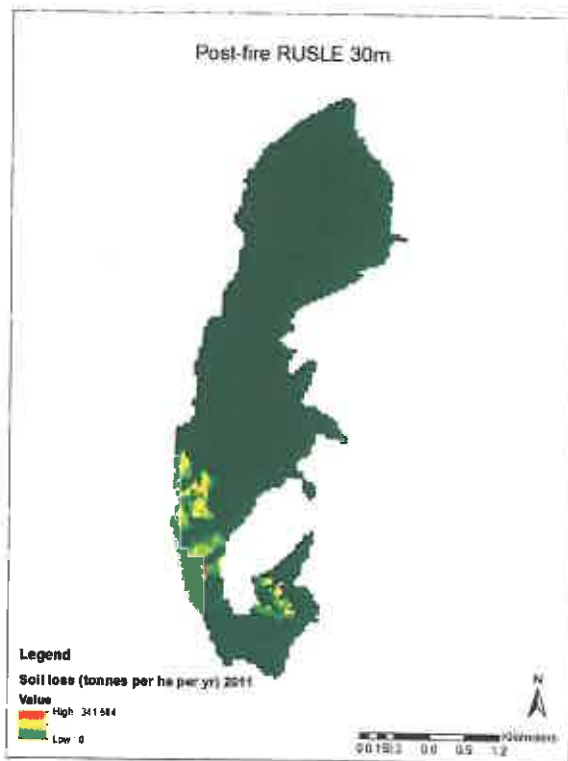


Figure 20. Unclassified post-fire soil loss

5.2 Water Quality

Water quality data for the Salinas watershed was acquired from the EPA STORET Central Warehouse database. Data from eight water quality sites was used. The locations of the water quality sites can be found in Figure 2a (aliases 2-5 and 7-10). Since the rainy season for the study area takes place during winter, water quality data including the months of December and January were collected and compared. The total dissolved solids (TDS) for December 2009-January 2010 were 435 mg/l, and total suspended solids (TSS) were 16 mg/l, for a total of 442 mg/l before the fire. TDS for December 2010-January 2011 were 556 mg/l, and TSS were 820 mg/l, for a total of 1,376 mg/l after the fire. Therefore, there was a total increase of 934 mg/l of dissolved and suspended solids during the rainy season following the Pozo wildfire compared to

before the fire. See Appendix B for a box and whisker plot of TDS and TSS data for the wet season before and the wet season after the fire. Appendix C is a table of the raw TDS and TSS data for the wet season before the fire which was used to create the ‘before’ box and whisker. Appendix D is a table of the raw TDS and TSS data for the wet season after the fire which was used to create the ‘after’ box and whisker. Appendix E shows a map of TDS stations (in orange) and TSS stations (in yellow).

Rainfall data was collected from NOAA Station ID #USC00047672 located in Salinas Dam (alias 12 in Figure 2a) and discharge data was collected from USGS Station ID #11147500 located in Paso Robles (alias 13 in Figure 2a) to see the relationship between rainfall and discharge (Figure 23). The location of the rainfall and discharge data stations can be found in Figure 2a. In addition, the relationship between monthly rainfall and monthly total solids found in the Salinas watershed rivers and streams can be seen in Figure 24.

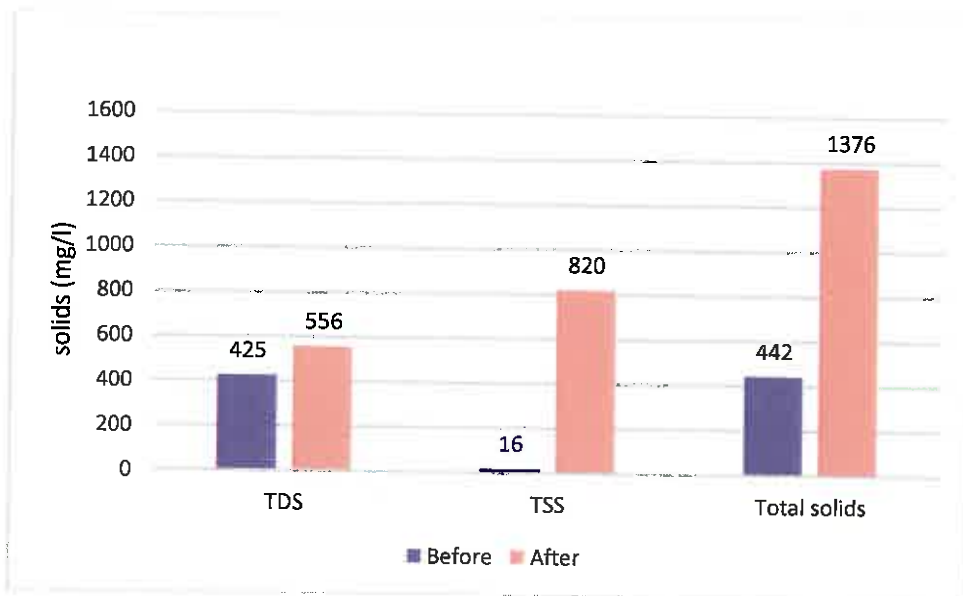


Figure 21. Average total suspended and dissolved solids before and after the fire

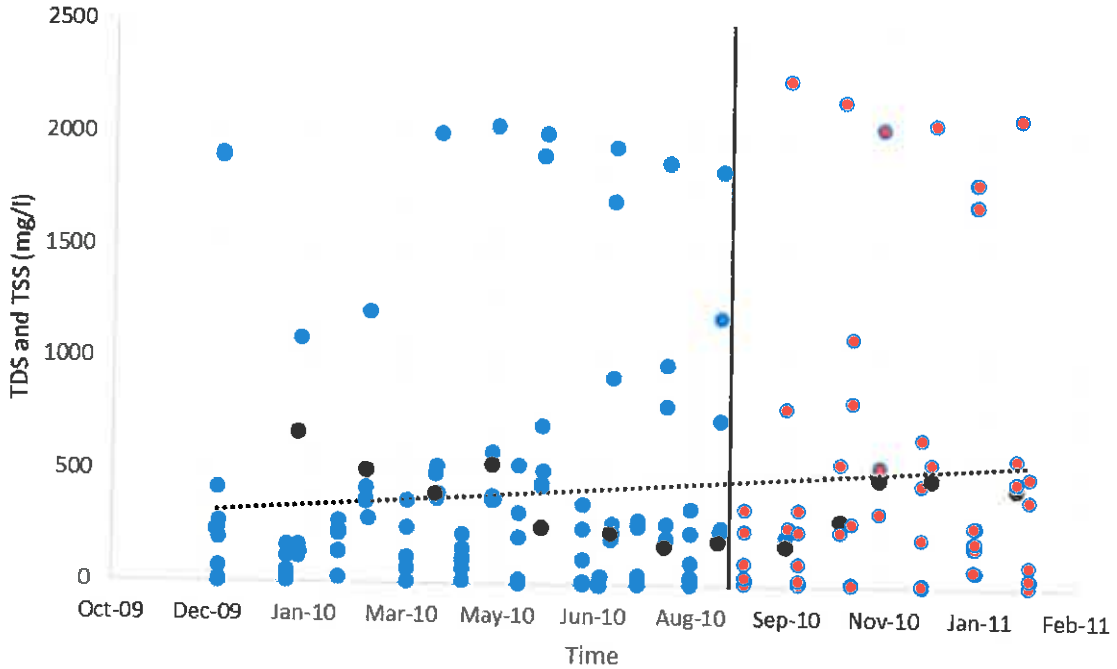


Figure 22. Time series of TDS and TSS (mg/l) from December 2009 (pre-fire: blue) to January 2011 (post-fire: red); Closest station (station alias 5): black

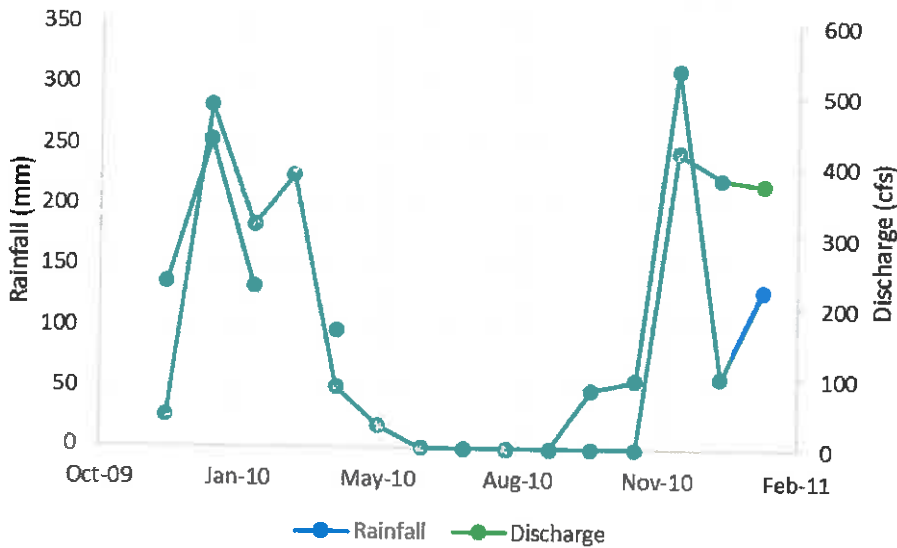


Figure 23. Monthly rainfall data (mm) collected from Station ID #UCS00047672 (NOAA) and monthly discharge data (cfs) collected from Station ID #11147500 (USGS)

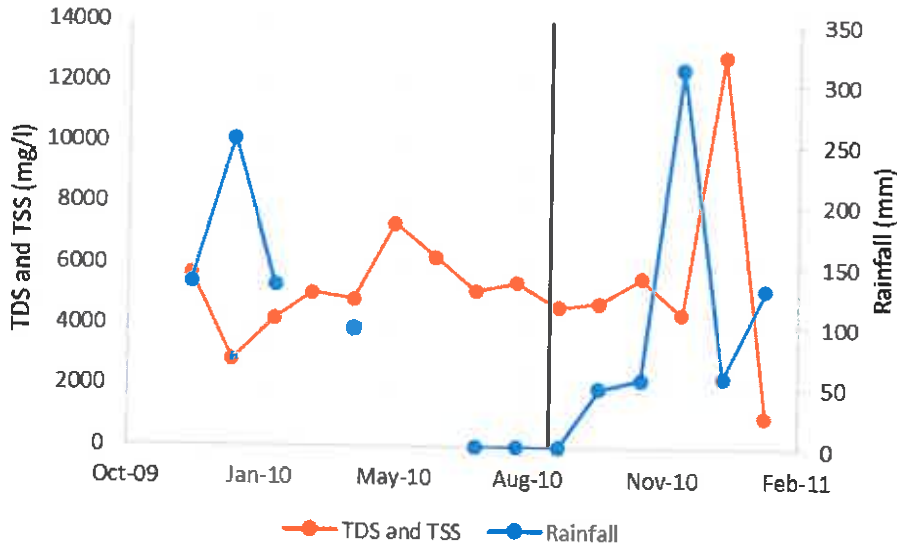


Figure 24. Monthly rainfall data (mm) from Station ID #USC00047672 (NOAA) and monthly water quality (solids) data from EPA STORET Salinas watershed using final 8 water quality sites

5.3 Impact of DEM Resolution on RUSLE Results

The 30m model yielded maximum soil loss values of 341 tonnes ha⁻¹ yr⁻¹ before and after the fire, while the 90m model yielded maximum soil loss values of 185 tonnes ha⁻¹ yr⁻¹ before the fire and 197 tonnes ha⁻¹ yr⁻¹ after the fire. In both cases, annual soil loss rate estimates produced by the 30m model were greater than the 90m model, and the maximum soil loss value for the post-fire 90m model was greater than the pre-fire 90m model by 6%.

Both the 30m and 90m analysis reported that the majority of the values (92-93%) were in the first class (low soil erosion risk potential). In pre-fire conditions, the first erosion class had the smallest difference in area between the DEM resolutions. The 30m model predicted 432.0 ha were in the first erosion class while the 90m model predicted 435.2 ha. The 90m model failed to report any area in the second class. Thus, the 30m model yielded an area greater than the 90m model by an order of magnitude of 3. The 30m model yielded 7.9 ha in the third erosion class while the 90m model yielded 4.2 ha. In the fourth class, the 30m model yielded 12.6 ha while the

90m model yielded 16.3. For the fifth class (high risk), the 30m model yielded 13.0 ha while the 90m model yielded 10.3 ha. On average, the 30m model yielded results with greater percent area in higher erosion classes.

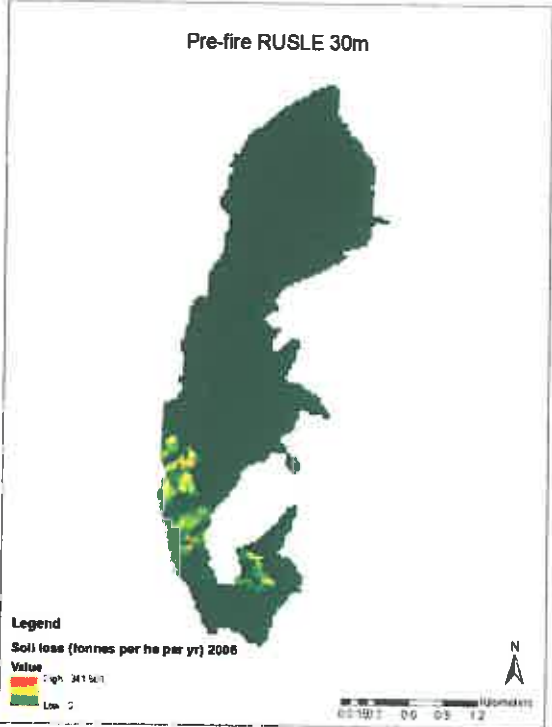


Figure 25. Unclassified pre-fire RUSLE map at 30m resolution

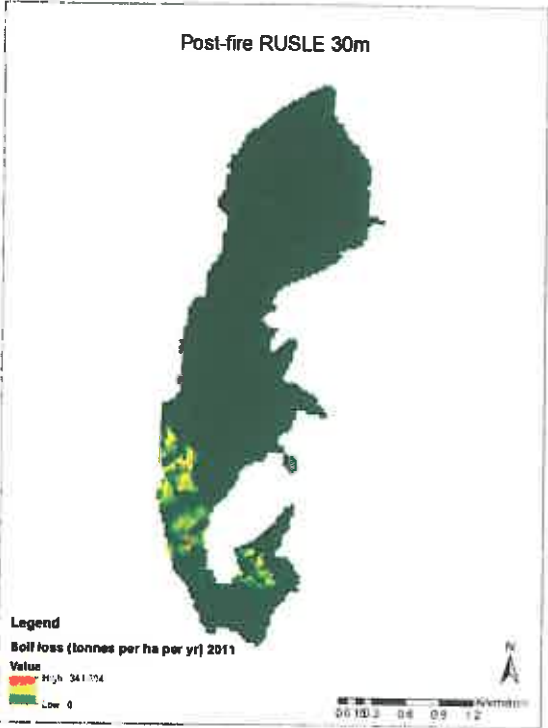


Figure 26. Unclassified post-fire RUSLE map at 30m resolution

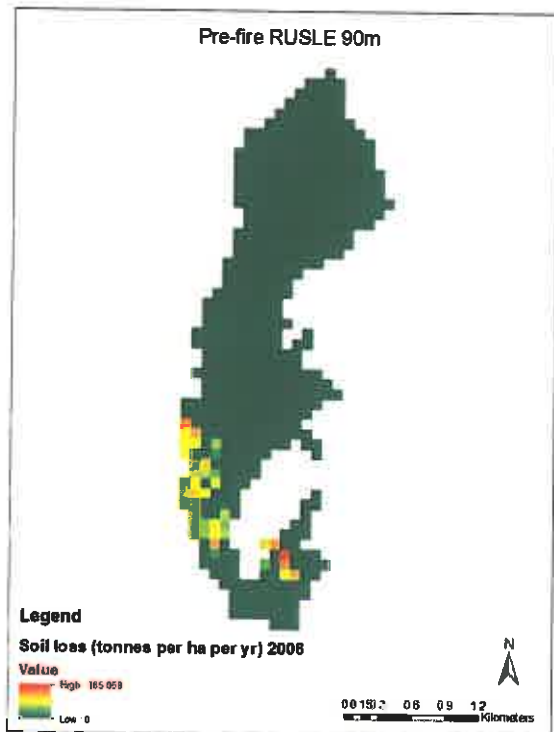


Figure 27. Unclassified pre-fire RUSLE map at 90m resolution

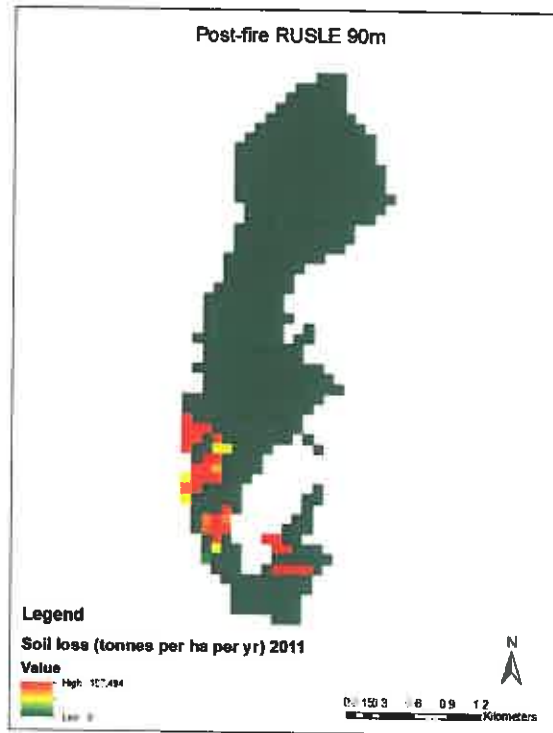


Figure 28. Unclassified post-fire RUSLE map at 90m resolution

Table 6. Pre- and post-fire maximum soil loss value (tonnes per hectare per year) comparison between resolution

	Pre-fire	Post-fire
Resolution	Max soil loss	Max soil loss
30m	341.6	341.6
90m	185.1	197.5

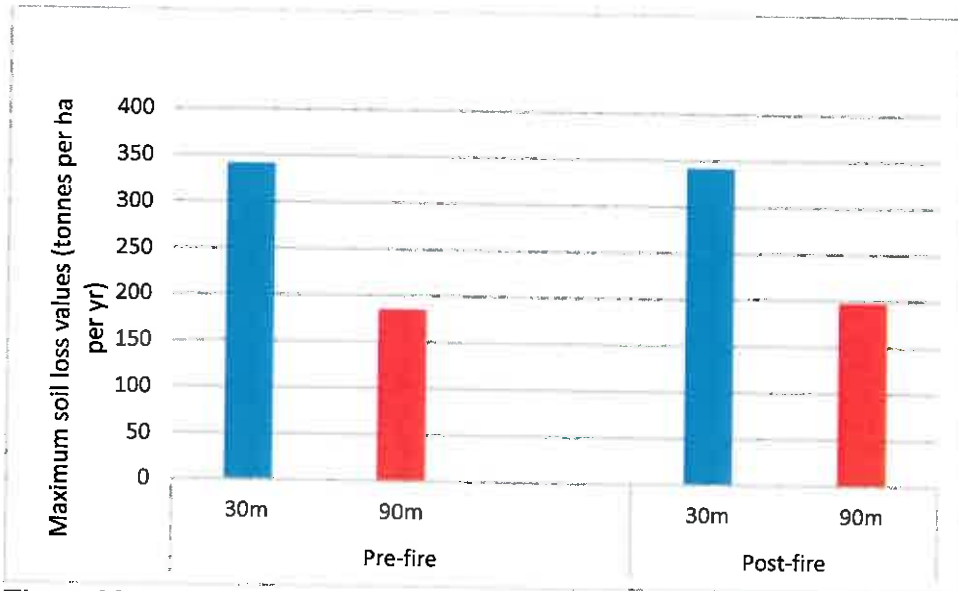


Figure 29. Pre- and post-fire maximum soil loss value (tonnes per hectare per year) comparison between resolutions

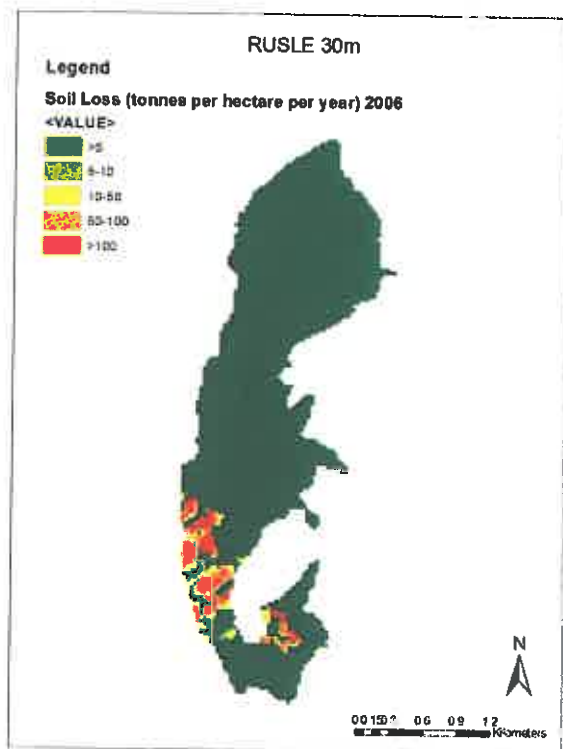


Figure 30. Classified pre-fire RUSLE map at 30m resolution

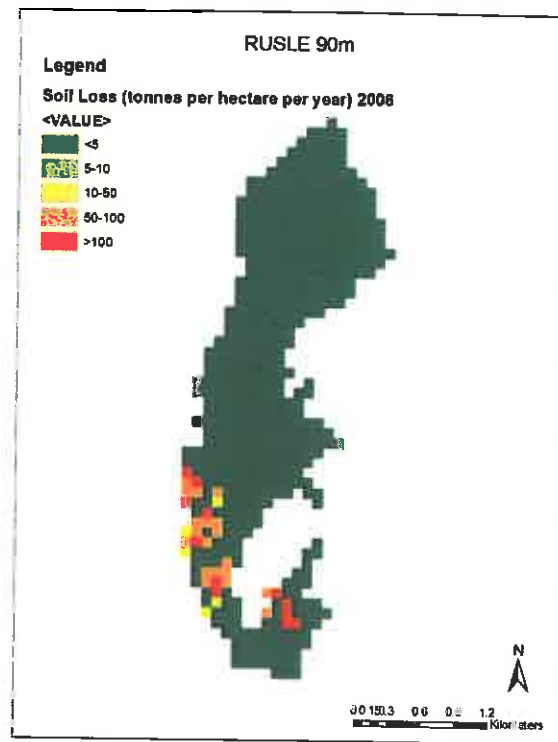


Figure 31. Classified pre-fire RUSLE at 90m resolution

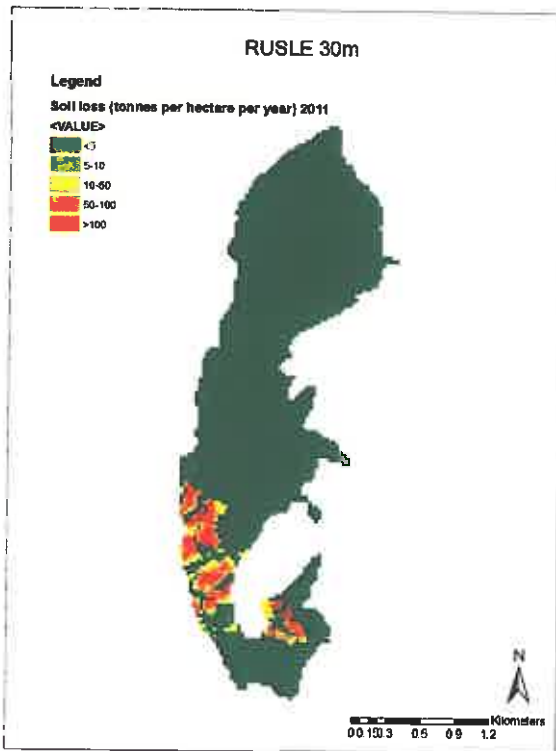


Figure 32. Classified post-fire RUSLE map at 30m resolution

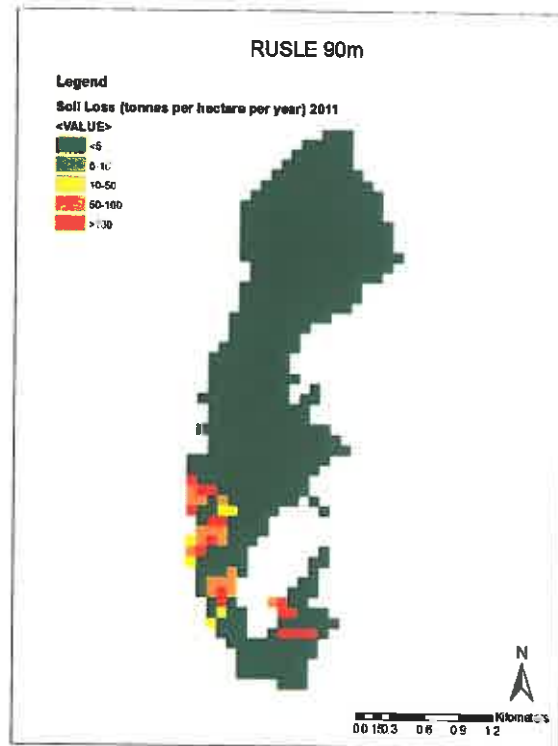


Figure 33. Classified post-fire RUSLE map at 90m resolution

Table 7. Pre- and post-fire erosion risk area coverage comparison between resolutions

Pre-fire			
	Erosion Risk	Percent Area	Area (ha)
30m	Low	92.7%	432.0
	Moderately Low	0.1%	0.5
	Moderate	1.7%	7.9
	Moderately High	2.7%	12.6
	High	2.8%	13.0
90m	Low	93.4%	435.2
	Moderately Low	0.0%	0.0
	Moderate	0.9%	4.2
	Moderately High	3.5%	16.3
	High	2.2%	10.3
Post-fire			
	Erosion Risk	Percent Area	Area (ha)
30m	Low	92.0%	428.7
	Moderately Low	0.1%	0.5
	Moderate	2.0%	9.3
	Moderately High	2.8%	13.0
	High	3.1%	14.4
90m	Low	92.6%	431.5
	Moderately Low	0.0%	0.0
	Moderate	1.1%	5.1
	Moderately High	3.1%	14.4
	High	3.1%	14.4

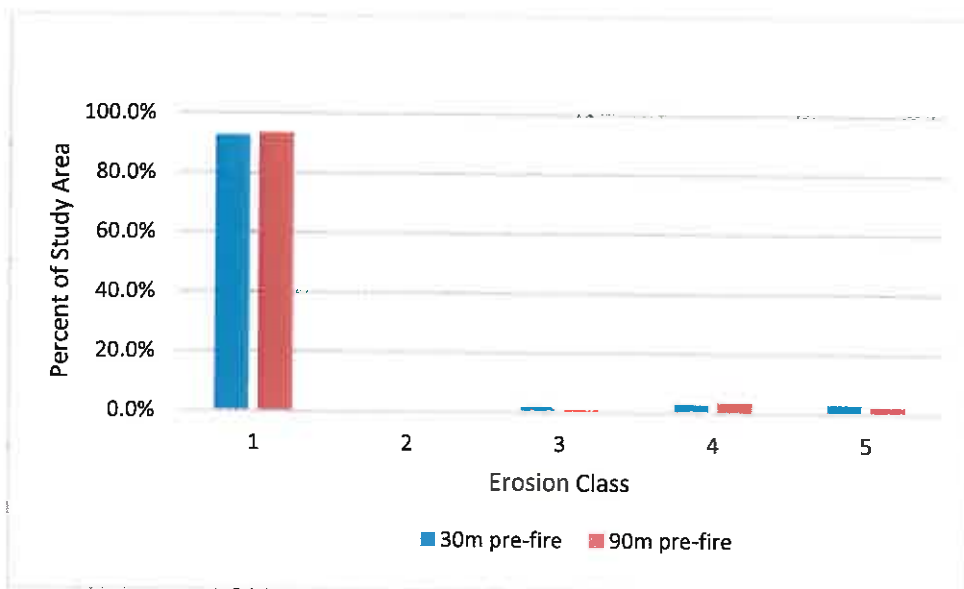


Figure 34. Pre-fire comparison of erosion class percent area between 30m and 90m resolution

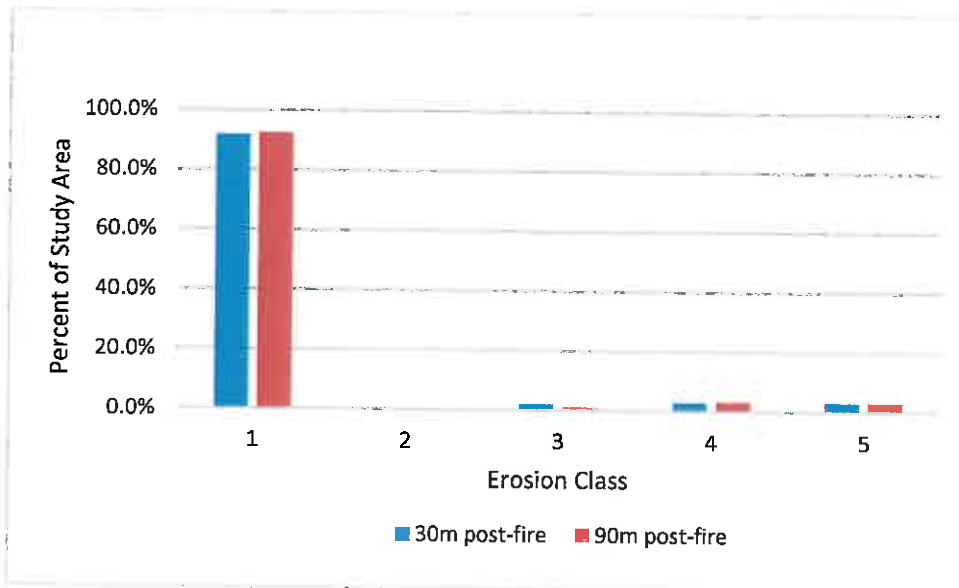


Figure 35. Post-fire comparison of erosion class percent area between 30m and 90m resolution

6 Discussion

The results of this study regarding the effect of fire on soil erosion are similar to the results of Mallinis et al. (2009), which found that heavy erosion classes covered 55% of the study area pre-fire and 90% of the study area post-fire. In both cases, the value of the maximum erosion rate estimation did not change after wildfire, but the percentage of high erosion classes did increase after the fire. Thus, wildfire did not seem to impact maximum soil loss rate values in the 30m model. Instead, the changes in the relative percent area of erosion classes was the most significant impact of wildfire. This distinction is important to note. While the maximum soil loss value did not increase after fire in the 30m model, the change in percentage of erosion classes to greater area coverage of high erosion classes means that erosion rates over the study area are, on average, expected to increase, resulting in an expected increase of total soil loss and therefore soil transport to nearby bodies of water.

While the results of this study are supported by those of other studies, empirically testing for accuracy of these results to determine error would be time-consuming, labor-intensive and

expensive. EPA water quality data for the Salinas watershed before and after the fire was used as a simple method of verifying the results. It was found that both TDS and TSS increased after the fire. However, it should be noted that TSS increased more than TDS after the fire (TDS increased by 131 mg/l while TSS increased by 804 mg/l). In addition, there were more TSS (820 mg/l) found after the fire than TDS (556 mg/l). This distinction is noteworthy because it indicates an increase in soil erosion by water and sediment transport to the water bodies in the Salinas watershed after the fire. Sediments carried by runoff after the fire would most likely be larger than 2 microns and would thus be classified as TSS as opposed to TDS (EPA 2012). TDS and TSS found in the Salinas watershed are a good indicator of soil erosion rates before and after the fire because soil particles that are detached are carried by surface runoff are likely to be transported to nearby streams or rivers. Since poor water quality is usually associated with high turbidity and high amounts of TDS and TSS, the increase in solids found after the fire support the results of the RUSLE analysis, which demonstrated an increase in area coverage of higher erosion risk potential classes. While an increase in TDS and TSS was found after the fire compared to before, without using source-tracking methods, it cannot be assumed that the increased in solids in the Salinas River was caused by the Pozo fire. However, these findings support the results of the RUSLE analysis, and the Pozo fire is one plausible explanation for this phenomenon. The fact that the Pozo fire took place in the headwater of the Salinas River further justifies this reasoning as it would have downstream impacts on water quality, and water quality stations downstream of the fire were used for data acquisition.

It should additionally be noted that the study area received 371 mm of rain in the December and January (wet season) immediately following the fire. This is significant in that San Luis Obispo County receives an *annual* mean of only 587 mm of precipitation. Therefore,

two months after the Pozo fire, San Luis Obispo County received 63% of the average annual rainfall. This is important because, as noted previously, the presence, absence and intensity of precipitation greatly impacts hydrological and sediment processes following a wildfire. If the fire occurs in the dry season, with little to no rain following the fire, erosion and sediment transport to nearby bodies of water is not to be expected and therefore, soil erosion may not be of concern. However, since the Pozo fire took place in late August, just months before the region's wet season, increased soil erosion after the fire was of greater concern, considering the amount of precipitation that followed. Figure 23 illustrates monthly rainfall (mm) and monthly discharge (cfs) data from December 2009 to February 2011. From the graph, it is clear that rainfall and discharge rose and fell together throughout the year and are therefore related. Discharge is the volumetric flow rate of water, including suspended solids and biological material in the water. Therefore, the spike in discharge in December 2010 and January 2011 is an indication of both increased precipitation due to the wet season and of the increase in TDS and TSS following the Pozo fire, evidenced in Figure 21.

Figure 24 illustrates the relationship between rainfall and TDS and TSS found in bodies of water in the Salinas watershed. The graph depicts a general correlation between rainfall and TDS and TSS, with TDS and TSS lagging slightly behind rainfall. The spike in rainfall (and then in TDS/TSS) in the few months following the fire has implications regarding soil erosion as precipitation drives the detachment of vulnerable sediments and the transportation of these sediments downstream. Since rainfall is the driver of erosion and TDS/TSS found in the water are the results of erosion, it explains why there is a lagging tendency of the TDS/TSS after the rainfall monthly data. As mentioned above, the rainfall, discharge and water quality stations used

are justified as the Pozo fire took place the Salinas River riverhead and the stations are located downstream (Figures 3 and 4).

The methods used could be improved through several modifications. The R value used in the RUSLE calculation was obtained from the isoerodent map in the NRCS Agriculture Handbook and is therefore an acceptable value. However, there are more accurate methods of R value calculation, including the method described in section 2.3.1, which uses total storm energy and maximum thirty-minute intensity data derived from rainfall data for the specific study area. In addition, the land cover data for pre- and post-fire was obtained from the NLCD 2006 and 2011 maps. The Pozo fire occurred in 2010. Since already classified yearly maps for California were not available, the NLCD 2006 and 2011 maps were used for pre- and post-fire respectively. While the 2006 NLCD map was the only available land cover map for the pre-fire study area, it was not a highly accurate representation of the study area directly before the fire. In the four years between 2006 and the Pozo fire (2010), the study area could have experienced land cover changes such as forest growth and land use changes due to development or agriculture. If significant forest growth took place between 2006 and 2010, then pre-fire soil erosion estimates may be overestimated, and the difference between pre- and post-fire erosion rates would be greater. A more accurate method for calculating the land management (C) factor is to use remotely sensed data to classify the land use/land cover of the study area directly before and after the Pozo fire. With this approach, “before” and “after” land cover data could be obtained for only a few days before and a few days after the fire, which could lead to more meaningful results. Appendix F contains a Landsat 7 satellite image of the study area a few days before the fire and was taken on August 15, 2010. Appendix G contains a Landsat 7 satellite image of the study area about a month after the fire and was taken on September 25, 2010.

The results regarding DEM resolution impact on RUSLE model outputs demonstrated that DEM resolution did have an impact on erosion rate estimates. At a coarser resolution (90m), the model underestimated erosion rates compared to the finer resolution (30m) (Table 6). While the 30m model did not detect changes in maximum soil loss rate before and after the fire, the 90m model predicted an increase in the value of the maximum soil loss rate after the fire. This may be due to uncertainty that resulted from resampling the land cover factor from 30m to 90m resolution. In addition, according to Figures 34 and 35, the percent coverage of the classes for the 30m and 90m model appear to be similar for both pre- and post-fire runs. This is, in part, due to the fact that the first class covered more than 90% of the study area in all cases, while the other classes covered less than 4%, making the scale of the graph very large and making it difficult to notice small differences. While the differences are small, on average, the finer resolution model predicted greater percent area in moderate to high erosion risk classes. Therefore, DEM resolution impacted almost exclusively the highest erosion values predicted by the model. These results support, to some extent, the results of others including Buakhao and Kangrang (2016), who demonstrated that DEM resolution impacts catchment area slope and stream network but that there is no significant advantage to using a finer resolution and Tan et al. (2015), who demonstrated that the SWAT model was most sensitive to DEM resolution, especially for smaller catchments. While these results demonstrate that DEM resolution has an impact on hydrological model results, choosing DEM resolution for future studies is a choice the model user must make and is dependent on several factors including the size of the research area, the scope of the research objectives and the availability of fine resolution data.

7 Conclusions

Forest fires have been a major concern for the state of California, especially in recent years due to a long drought. Of particular concern are the possibly dangerous implications following forest fires, including land degradation, increased soil erosion and mudslides. This study used a GIS model to estimate soil loss before and after the Pozo wildfire of 2010 to determine the effect of wildfire on soil erosion. Percentage of erosion hot spots increased from 5.5% of the study area before the fire to 5.9% after the fire for the 30m model. Moderate risk potential area coverage increased from 2.0% to 2.7% after the fire. These results suggest that the Pozo wildfire led to moderate increases in erosion risk potential for the study area. Water quality data from the Salinas watershed verified the results from the RUSLE model. The average total dissolved solids found in the Salinas watershed increased by 131 mg/l after the fire, and average total suspended solids increased by 804 mg/l after the fire. Therefore, there was a total increase of 934 mg/l for dissolved and suspended solids in the wet season after the Pozo fire compared to before, suggesting that the Pozo wildfire did have an environmental impact on the surrounding hydrological system by increasing soil erosion and sediment transport to nearby bodies of water. While the Pozo fire is one plausible explanation for this increase, without using source-tracking methods, it cannot be assumed that the fire was the cause of this increase. Instead, the water quality results were used simply to verify RUSLE results. Planners and modelers may use similar methods to prioritize watershed protection and mitigation efforts following future wildfires.

This study also examined the effect of DEM resolution on RUSLE results. On average, the 30m model estimates of annual soil erosion were greater than the 90m model estimates. The maximum annual soil loss value yielded by the 30m model was 341 tonnes ha⁻¹ yr⁻¹ for both pre- and post-fire models, while the 90m model yielded a maximum value of 185 tonnes ha⁻¹ yr⁻¹ for

pre-fire and 197 tonnes ha⁻¹ yr⁻¹ for post-fire. Based on the results of this study, soil erosion models using coarser resolution DEM data can underestimate maximum soil loss rates and soil erosion risk potential for some erosion classes. However, it is up to model users to determine if the difference is significant enough to warrant the use of finer resolution data when available, sometimes at a greater cost.

7 References

- Accuweather. (2017, December 8). *AccuWeather predicts 2017 California wildfire season cost to rise to \$180 billion*. Retrieved from <https://www.accuweather.com/en/weather-news/accuweather-predicts-2017-california-wildfire-season-cost-to-rise-to-180-billion/70003495>
- Aksoy, H., & Kavvas, M. L. (2005). A review of hillslope and watershed scale erosion and sediment transport models. *Catena*, 64(2), 247-271.
- Amezketta, E. (1999). Soil aggregate stability: a review. *Journal of sustainable agriculture*, 14(2-3), 83-151.
- Anderson, J. R. (1976). *A land use and land cover classification system for use with remote sensor data* (Vol. 964). Washington, DC: U.S. Government Printing Office.
- Benavides-Solorio, J., & MacDonald, L. H. (2001). Post-fire runoff and erosion from simulated rainfall on small plots, Colorado Front Range. *Hydrological Processes*, 15(15), 2931-2952.
- Bilotta, G. S., & Brazier, R. E. (2008). Understanding the influence of suspended solids on water quality and aquatic biota. *Water Research*, 42(12), 2849-2861.

- Buakhao, W., & Kangrang, A. (2016). DEM resolution impact on the estimation of the physical characteristics of watersheds by using SWAT. *Advances in Civil Engineering*, 2016.
- Byram, G. M. (1959). Combustion of forest fuels. *Forest fire: control and use*, 61-89.
- CAL FIRE. (2016, September 23). *Fire Statistics*. Retrieved from http://cdfdata.fire.ca.gov/incidents/incidents_stats?year=2017
- California Department of Forestry and Fire Protection. (2010, August 21). *The Pozo Fire*. Retrieved from <http://www.fire.ca.gov/downloads/incidents/2010/PozoFire8-21.pdf>
- Cerdà, A., & Robichaud, P. (2009). Fire effects on soil infiltration. *Fire effects on soils and restoration strategies* (pp. 81-103). Boca Raton, FL: Science Publishers.
- Cheney, N. P. (1981). Fire behaviour. *Fire and the Australian Biota*. (Eds AM Gill, RH Groves, IR Noble) pp, 151-175.
- Claessens, L., Heuvelink, G. B. M., Schoorl, J. M., & Veldkamp, A. (2005). DEM resolution effects on shallow landslide hazard and soil redistribution modelling. *Earth Surface Processes and Landforms*, 30(4), 461-477.
- Daly, C., Neilson, R. P., & Phillips, D. L. (1994). A statistical-topographic model for mapping climatological precipitation over mountainous terrain. *Journal of applied meteorology*, 33(2), 140-158.
- De Luis, M., González-Hidalgo, J. C., & Raventós, J. (2003). Effects of fire and torrential rainfall on erosion in a Mediterranean gorse community. *Land Degradation & Development*, 14(2), 203-213.
- DeBano, L. F., Neary, D. G., & Ffolliott, P. F. (1998). *Fire effects on ecosystems*. New York, NY: John Wiley & Sons Inc.

- Doerr, S. H., Shakesby, R. A., Blake, W. H., Chafer, C. J., Humphreys, G. S., & Wallbrink, P. J. (2006). Effects of differing wildfire severities on soil wettability and implications for hydrological response. *Journal of Hydrology*, 319(1), 295-311.
- Dragovich, D., & Morris, R. (2002). Fire intensity, slopewash and bio-transfer of sediment in eucalypt forest, Australia. *Earth Surface Processes and Landforms*, 27(12), 1309-1319.
- Dunin, F. X. (1976). Infiltration: Its simulation for field conditions. *Facets of hydrology*.
- EPA. (2012). 5.5 Turbidity. In *Water: Monitoring & Assessment*. Retrieved from <http://water.epa.gov/type/rsll/monitoring/vms55.cfm>
- Forrest, C. L., & Harding, M. V. (1994). Erosion and sediment control: preventing additional disasters after the southern California fires. *Journal of Soil and Water Conservation*, 49(6), 535-541.
- Foster, G. R., McCool, D. K., Renard, K. G., & Moldenhauer, W. C. (1981). Conversion of the universal soil loss equation to SI metric units. *Journal of Soil and Water Conservation*, 36(6), 355-359.
- Gallant, J. (2001). Topographic scaling for the NLWRA sediment project. *CSIRO Land and Water*.
- Gao, J. (1998). Impact of sampling intervals on the reliability of topographic variables mapped from grid DEMs at a micro-scale. *International Journal of Geographical Information Science*, 12(8), 875-890.
- Gardiner, E. P., & Meyer, J. L. (2001). Sensitivity of RUSLE to Data Resolution: Modeling Sediment Delivery in Upper Little Tennessee River Basin. Georgia Institute of Technology.

- Guerrero, C., Mataix-Solera, J., Navarro-Pedreño, J., García-Orenes, F., & Gómez, I. (2001). Different patterns of aggregate stability in burned and restored soils. *Arid Land Research and Management*, 15(2), 163-171.
- Hartford, R. A., & Frandsen, W. H. (1992). When it's hot, it's hot... or maybe it's not!(Surface flaming may not portend extensive soil heating). *International Journal of Wildland Fire*, 2(3), 139-144.
- Henderson, G. S., & Golding, D. L. (1983). The effect of slash burning on the water repellency of forest soils at Vancouver, British Columbia. *Canadian Journal of Forest Research*, 13(2), 353-355.
- Hoetzel, S., Dupont, L., Schefuß, E., Rommerskirchen, F., & Wefer, G. (2013). The role of fire in Miocene to Pliocene C4 grassland and ecosystem evolution. *Nature Geoscience*, 6(12), 1027.
- Huffman, E. L., MacDonald, L. H., & Stednick, J. D. (2001). Strength and persistence of fire-induced soil hydrophobicity under ponderosa and lodgepole pine, Colorado Front Range. *Hydrological Processes*, 15(15), 2877-2892.
- Imeson, A. C., Verstraten, J. M., Van Mulligen, E. J., & Sevink, J. (1992). The effects of fire and water repellency on infiltration and runoff under Mediterranean type forest. *Catena*, 19(3-4), 345-361.
- Kokaly, R. F., Rockwell, B. W., Haire, S. L., & King, T. V. (2007). Characterization of post-fire surface cover, soils, and burn severity at the Cerro Grande Fire, New Mexico, using hyperspectral and multispectral remote sensing. *Remote Sensing of Environment*, 106(3), 305-325.

- Kutiel, P., Lavee, H., Segev, M., & Benyamini, Y. (1995). The effect of fire-induced surface heterogeneity on rainfall-runoff-erosion relationships in an eastern Mediterranean ecosystem, Israel. *Catena*, 25(1), 77-87.
- Lisenby, P. E., & Fryirs, K. A. (2017). 'Out with the Old?' Why coarse spatial datasets are still useful for catchment-scale investigations of sediment (dis)connectivity. *Earth Surface Processes & Landforms*, 42(10), 1588-1596.
- Mallinis, G., Maris, F., Kalinderis, I., & Koutsias, N. (2009). Assessment of Post-fire Soil Erosion Risk in Fire-Affected Watersheds Using Remote Sensing and GIS. *Geoscience And Remote Sensing*, 46(4), 388-410.
- Mallinis, G., Gitas, I. Z., Tasionas, G., & Maris, F. (2016). Multitemporal monitoring of land degradation risk Due to soil loss in a fire-prone Mediterranean landscape using multi-decadal Landsat imagery. *Water resources management*, 30(3), 1255-1269.
- Miller, M. E., Elliot, W. J., Billmire, M., Robichaud, P. R., & Endsley, K. A. (2016). Rapid-response tools and datasets for post-fire remediation: linking remote sensing and process-based hydrological models. *International Journal of Wildland Fire*, 25(10), 1061-1073.
- Miller, J. D., Nyhan, J. W., & Yool, S. R. (2003). Modeling potential erosion due to the Cerro Grande Fire with a GIS-based implementation of the Revised Universal Soil Loss Equation. *International Journal of Wildland Fire*, 12(1), 85-100.
- Millward, A. A., & Mersey, J. E. (1999). Adapting the RUSLE to model soil erosion potential in a mountainous tropical watershed. *Catena*, 38(2), 109-129.
- Mitra, B., Scott, H. D., Dixon, J. C., & McKimmey, J. M. (1998). Applications of fuzzy logic to the prediction of soil erosion in a large watershed. *Geoderma*, 86(3-4), 183-209.

- Moritz, M. A. (1997). Analyzing extreme disturbance events: fire in Los Padres National Forest. *Ecological Applications*, 7(4), 1252-1262.
- Morton, F. I. (1983). Operational estimates of areal evapotranspiration and their significance to the science and practice of hydrology. *Journal of Hydrology*, 66(1-4), 1-76.
- Mutch, R. W. (1970). Wildland Fires and Ecosystems--A Hypothesis. *Ecology*, 51(6), 1046-1051.
- National Oceanic and Atmospheric Administration. (2010). *1981-2010 Normals* [Data file]. Retrieved from <https://www.ncdc.noaa.gov/cdo-web/datatools/normals>
- NBC Bay Area. (2018, January 9). *13 Killed as Mudslides Hit Wildfire-Ravaged SoCal*. Retrieved from <https://www.nbcbayarea.com/news/california/Explosion-Debris-Flow-Reported-After-House-Fire-in-Montecito-468430023.html>
- Neary, D. G., Klopatek, C. C., DeBano, L. F., & Ffolliott, P. F. (1999). Fire effects on belowground sustainability: a review and synthesis. *Forest ecology and management*, 122(1), 51-71.
- Passalacqua, P., Belmont, P., Staley, D. M., Simley, J. D., Arrowsmith, J. R., Bode, C. A., ... & Lague, D. (2015). Analyzing high resolution topography for advancing the understanding of mass and energy transfer through landscapes: A review. *Earth-Science Reviews*, 148, 174-193.
- Prodanović, D., Stanić, M., Milivojević, V., Simić, Z., & Arsić, M. (2009). DEM-based GIS algorithms for automatic creation of hydrological models data. *J Serbian Soc Computation Mech*, 3(1), 64-85.
- Prosser, I. P., & Williams, L. (1998). The effect of wildfire on runoff and erosion in native Eucalyptus forest. *Hydrological processes*, 12(2), 251-265.

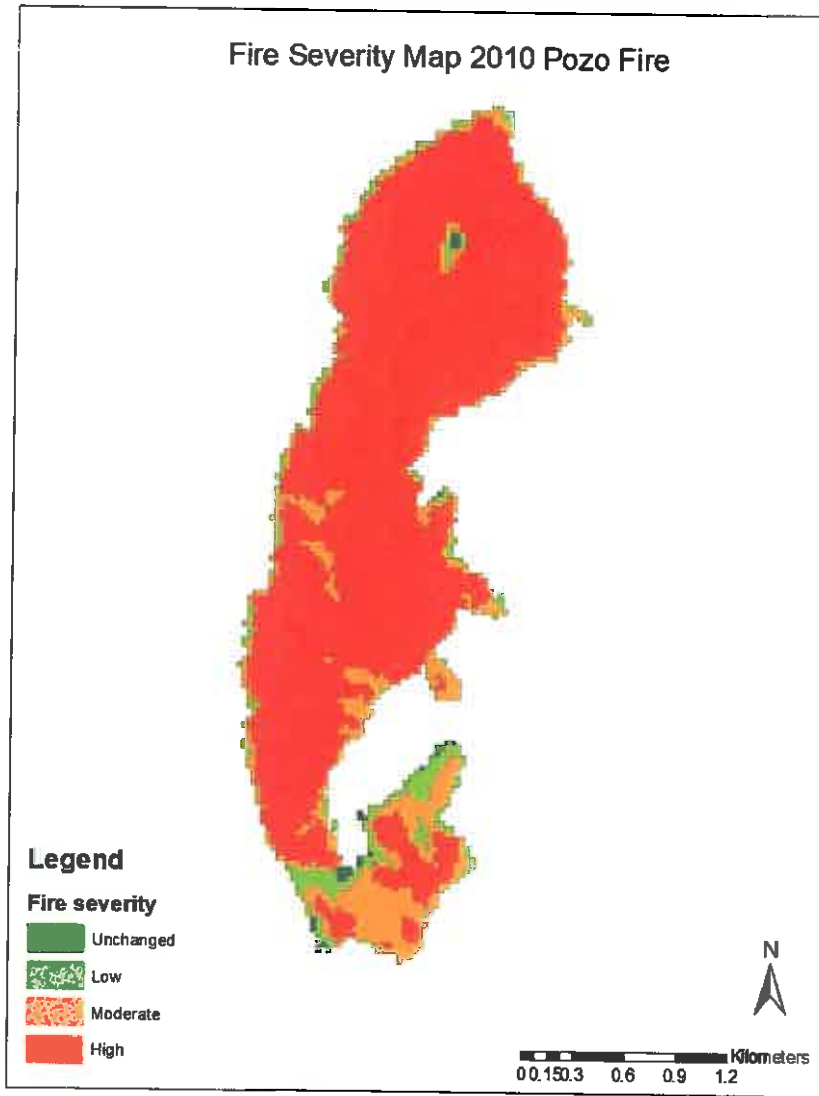
- Robichaud, P. R., & Ashmun, L. E. (2013). Tools to aid post-wildfire assessment and erosion-mitigation treatment decisions. *International Journal of Wildland Fire*, 22(1), 95-105.
- Robichaud, P. R., & Hungerford, R. D. (2000). Water repellency by laboratory burning of four northern Rocky Mountain forest soils. *Journal of Hydrology*, 231, 207-219.
- Robichaud, P. R., & Miller, S. M. (1999). Spatial interpolation and simulation of post-burn duff thickness after prescribed fire. *International Journal of Wildland Fire*, 9(2), 137-143.
- Samantha Raphelson. (2018, January 12). *Southern California Hillsides Remain Vulnerable After Deadly Mudslides*. Retrieved from <https://www.npr.org/2018/01/12/577671170/southern-california-hillsides-remain-vulnerable-after-deadly-mudslides>
- Santa Maria Times. (2010, August 22). *Firefighters report progress on Pozo fire*. Retrieved from http://santamariatimes.com/news/local/firefighters-report-progress-on-pozo-fire/article_8be4e060-ae5a-11df-b664-001cc4c002e0.html
- Schoennagel, T., Smithwick, E. A., & Turner, M. G. (2009). Landscape heterogeneity following large fires: insights from Yellowstone National Park, USA. *International Journal of Wildland Fire*, 17(6), 742-753.
- Schoorl, J. M., Sonneveld, M. P. W., & Veldkamp, A. (2000). Three-dimensional landscape process modelling: the effect of DEM resolution. *Earth Surface Processes and Landforms*, 25(9), 1025-1034.
- Scott, D. F., & Van Wyk, D. B. (1990). The effects of wildfire on soil wettability and hydrological behaviour of an afforested catchment. *Journal of hydrology*, 121(1), 239-256.

- Shakesby, R. A., Chafer, C. J., Doerr, S. H., Blake, W. H., Wallbrink, P., Humphreys, G. S., & Harrington, B. A. (2003). Fire severity, water repellency characteristics and hydrogeomorphological changes following the Christmas 2001 Sydney forest fires. *Australian Geographer*, 34(2), 147-175.
- Shakesby, R. A., & Doerr, S. H. (2006). Wildfire as a hydrological and geomorphological agent. *Earth-Science Reviews*, 74(3), 269-307.
- Smith, R. E., & Goodrich, D. C. (2006). Rainfall excess overland flow. In *Encyclopedia of Hydrological Sciences*. (Vol. 1, pp. 1707-1718). New York, NY: John Wiley & Sons Inc.
- Summerfield, M. A. (1991). *Global geomorphology: An introduction to the study of landforms*. Pearson Education Limited.
- Tan, M. L., Ficklin, D. L., Dixon, B., Yusop, Z., & Chaplot, V. (2015). Impacts of DEM resolution, source, and resampling technique on SWAT-simulated streamflow. *Applied Geography*, 63, 357-368.
- Thompson, J. A., Bell, J. C., & Butler, C. A. (2001). Digital elevation model resolution: effects on terrain attribute calculation and quantitative soil-landscape modeling. *Geoderma*, 100(1), 67-89.
- United States Department of Agriculture. (1978). *Predicting Rainfall Erosion Losses: A Guide to Conservation Planning* (Agricultural Handbook No. 537). Washington, DC: U.S. Government Printing Office.
- United States Department of Agriculture. (1997). *Predicting soil erosion by water: a guide to conservation planning with the revised universal soil loss equation (RUSLE)* (Agricultural Handbook No. 703). Washington, DC: U.S. Government Printing Office.

- Vafeidis, A. T., Drake, N. A., & Wainwright, J. (2007). A proposed method for modelling the hydrologic response of catchments to burning with the use of remote sensing and GIS. *Catena*, 70(3), 396-409.
- Wilson, C. J., Carey, J. W., Beeson, P. C., Gard, M. O., & Lane, L. J. (2001). A GIS-based hillslope erosion and sediment delivery model and its application in the Cerro Grande burn area. *Hydrological Processes*, 15(15), 2995-3010.
- Wischmeier, W. H. & Smith, D.D.(1978). Predicting Rainfall Erosion Losses: A Guide to Conservation Planning. *U.S. Department of Agriculture, Agriculture Handbook No. 537*.
- Wise, S. (2000). Assessing the quality for hydrological applications of digital elevation models derived from contours. *Hydrological processes*, 14(11-12), 1909-1929.
- Wondzell, S.M. (2001). The influence of forest health and protection treatments on erosion and stream sedimentation in forested watersheds of eastern Oregon and Washington. *Northwest Science*, 75, 128-140.
- Zhou, Y., Zhang, Y., Vaze, J., Lane, P., & Xu, S. (2013). Improving runoff estimates using remote sensing vegetation data for bushfire impacted catchments. *Agricultural and forest meteorology*, 182, 332-341.
- Zhang, J. X., Chang, K. T., & Wu, J. Q. (2008). Effects of DEM resolution and source on soil erosion modelling: A case study using the WEPP model. *International Journal of Geographical Information Science*, 22(8), 925-942.
- Zhang, Y., Chiew, F. H., Zhang, L., & Li, H. (2009). Use of remotely sensed actual evapotranspiration to improve rainfall–runoff modeling in Southeast Australia. *Journal of Hydrometeorology*, 10(4), 969-980.

Appendix A

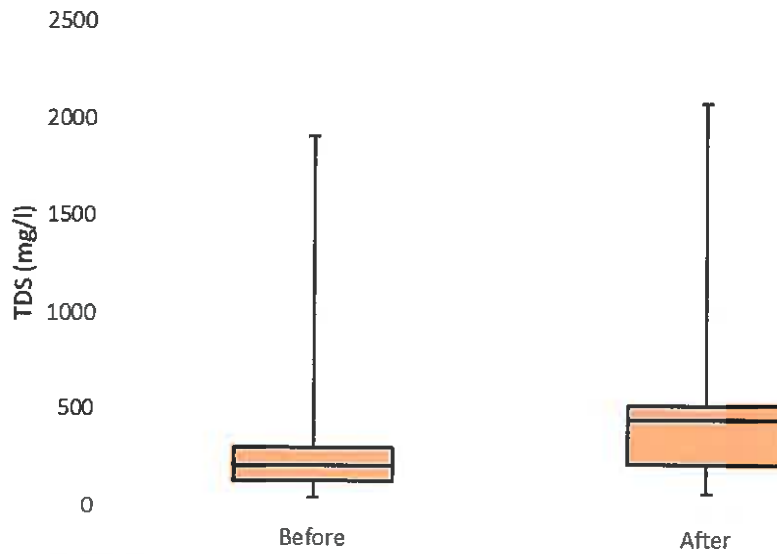
Fire Severity Map



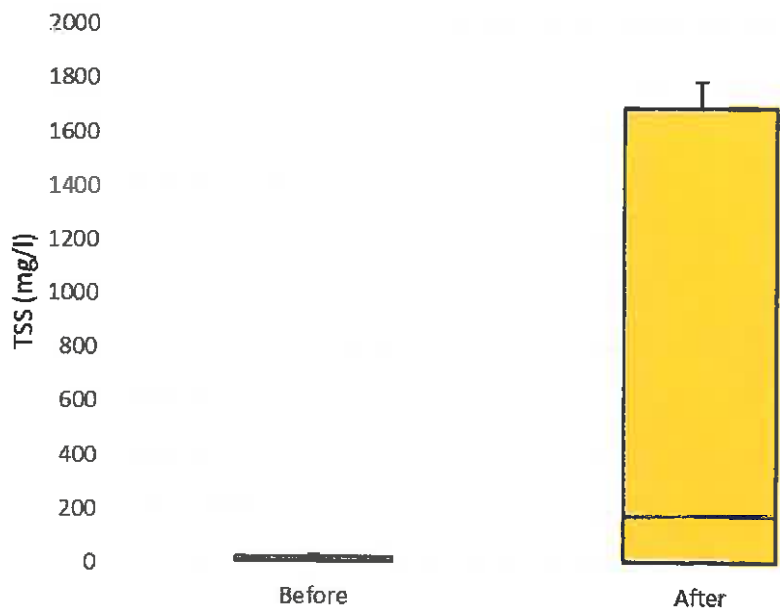
Percent Area of Fire Severity Classes

Fire Severity Class	Percent Area
Unchanged	25.8%
Low	16.0%
Moderate	35.3%
High	22.9%

Appendix B



Box and Whisker Plot for TDS in wet season before versus wet season after the 2010 Pozo fire



Box and Whisker Plot for TSS in wet season before versus wet season after the 2010 Pozo fire

Appendix C

Raw TDS and TSS Data for Wet Season Before Pozo 2010 Fire (December 2009 – January 2010)

Station ID	HUC	Latitude	Longitude	Activity Start	Characteristic Description	Value	Units
309GRN	18060005	36.3377	-121.205	12/7/2009	Total dissolved solids~Dissolved~CEDEN~49~mg/l	230	mg/l
309SAG	18060005	36.4863	-121.47	12/7/2009	Total dissolved solids~Dissolved~CEDEN~49~mg/l	230	mg/l
309SAC	18060005	36.5538	-121.548	12/7/2009	Total dissolved solids~Dissolved~CEDEN~49~mg/l	240	mg/l
309QUI	18060005	36.6096	-121.561	12/7/2009	Total dissolved solids~Dissolved~CEDEN~49~mg/l	420	mg/l
309SSP	18060005	36.629	-121.688	12/7/2009	Total dissolved solids~Dissolved~CEDEN~49~mg/l	230	mg/l
309DAV	18060005	36.6468	-121.701	12/8/2009	Total suspended solids~CEDEN~7~mg/l	13	mg/l
309DAV	18060005	36.6468	-121.701	12/8/2009	Total suspended solids~Fixed~CEDEN~234~mg/l	8.9	mg/l
309DAV	18060005	36.6468	-121.701	12/8/2009	Total suspended solids~Volatile~CEDEN~234~mg/l	3.8	mg/l
309DAV	18060005	36.6468	-121.701	12/8/2009	Total dissolved solids~Volatile~CEDEN~234~mg/l	72	mg/l
309DAV	18060005	36.6468	-121.701	12/8/2009	Total dissolved solids~Dissolved~CEDEN~6~mg/l	270	mg/l
309DAV	18060005	36.6468	-121.701	12/8/2009	Total dissolved solids~Fixed~CEDEN~234~mg/l	200	mg/l
309BLA	18060005	36.7085	-121.749	12/8/2009	Total dissolved solids~Dissolved~CEDEN~49~mg/l	1910	mg/l
309BLA	18060005	36.7085	-121.749	12/8/2009	Total dissolved solids~Dissolved~CEDEN~49~mg/l	1900	mg/l
309DAV	18060005	36.6468	-121.701	1/12/2010	Total suspended solids~Fixed~CEDEN~234~mg/l	28	mg/l
309DAV	18060005	36.6468	-121.701	1/12/2010	Total suspended solids~Volatile~CEDEN~234~mg/l	9.5	mg/l
309DAV	18060005	36.6468	-121.701	1/12/2010	Total suspended solids~CEDEN~7~mg/l	38	mg/l
309DAV	18060005	36.6468	-121.701	1/12/2010	Total dissolved solids~Volatile~CEDEN~234~mg/l	53	mg/l
309DAV	18060005	36.6468	-121.701	1/12/2010	Total dissolved solids~Dissolved~CEDEN~6~mg/l	170	mg/l
309DAV	18060005	36.6468	-121.701	1/12/2010	Total dissolved solids~Fixed~CEDEN~234~mg/l	120	mg/l
309GRN	18060005	36.3377	-121.205	1/18/2010	Total dissolved solids~Dissolved~CEDEN~49~mg/l	670	mg/l
309SAG	18060005	36.4863	-121.47	1/18/2010	Total dissolved solids~Dissolved~CEDEN~49~mg/l	119	mg/l
309SAC	18060005	36.5538	-121.548	1/18/2010	Total dissolved solids~Dissolved~CEDEN~49~mg/l	139	mg/l
309CRR	18060005	36.5638	-121.514	1/18/2010	Total dissolved solids~Dissolved~CEDEN~49~mg/l	167	mg/l
309QUI	18060005	36.6096	-121.561	1/18/2010	Total dissolved solids~Dissolved~CEDEN~49~mg/l	139	mg/l
309SSP	18060005	36.629	-121.688	1/19/2010	Total dissolved solids~Dissolved~CEDEN~49~mg/l	135	mg/l
309BLA	18060005	36.7085	-121.749	1/19/2010	Total dissolved solids~Dissolved~CEDEN~49~mg/l	1090	mg/l

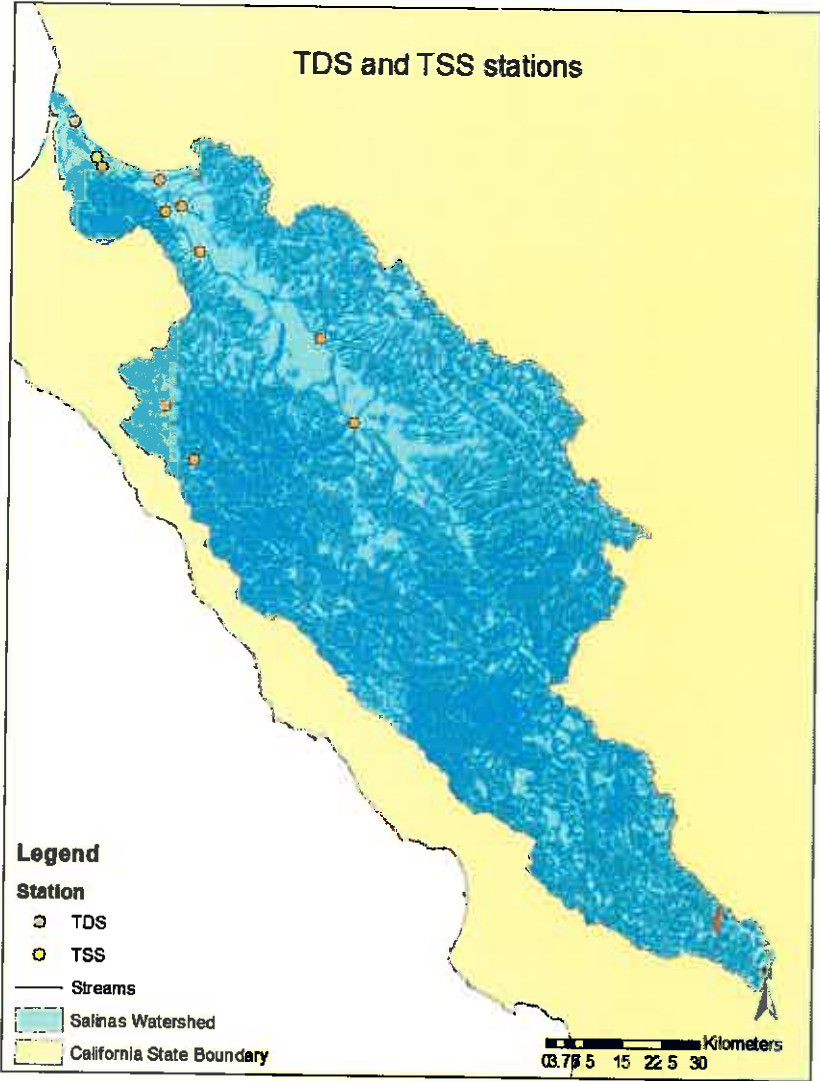
Appendix D

Raw TDS and TSS Data for Wet Season After Pozo 2010 Fire (December 2010 – January 2011)

Station ID	HUC	Latitude	Longitude	Activity Start	Characteristic Description	Value	Units
309DAV	18060005	36.6468	-121.701	12/7/2010	Total suspended solids~Fixed~CEDEN~234~mg/l	7.8	mg/l
309DAV	18060005	36.6468	-121.701	12/7/2010	Total suspended solids~CEDEN~7~mg/l	12	mg/l
309DAV	18060005	36.6468	-121.701	12/7/2010	Total suspended solids~Volatile~CEDEN~234~mg/l	4.8	mg/l
309DAV	18060005	36.6468	-121.701	12/7/2010	Total dissolved solids~Dissolved~CEDEN~6~mg/l	660	mg/l
309DAV	18060005	36.6468	-121.701	12/7/2010	Total dissolved solids~Volatile~CEDEN~234~mg/l	210	mg/l
309DAV	18060005	36.6468	-121.701	12/7/2010	Total dissolved solids~Fixed~CEDEN~234~mg/l	450	mg/l
309GRN	18060005	36.3377	-121.205	12/12/2010	Total dissolved solids~Dissolved~CEDEN~49~mg/l	483	mg/l
309SAG	18060005	36.4863	-121.47	12/12/2010	Total dissolved solids~Dissolved~CEDEN~49~mg/l	546	mg/l
309BLA	18060005	36.7085	-121.749	12/13/2010	Total dissolved solids~Dissolved~CEDEN~49~mg/l	2060	mg/l
309DAV	18060005	36.6468	-121.701	1/3/2011	Total suspended solids~CEDEN~234~mg/l	1700	mg/l
309DAV	18060005	36.6468	-121.701	1/3/2011	Total suspended solids~Volatile~CEDEN~234~mg/l	180	mg/l
309DAV	18060005	36.6468	-121.701	1/3/2011	Total suspended solids~CEDEN~7~mg/l	1800	mg/l
309DAV	18060005	36.6468	-121.701	1/3/2011	Total dissolved solids~CEDEN~234~mg/l	200	mg/l
309DAV	18060005	36.6468	-121.701	1/3/2011	Total dissolved solids~Dissolved~CEDEN~6~mg/l	270	mg/l
309DAV	18060005	36.6468	-121.701	1/3/2011	Total dissolved solids~Volatile~CEDEN~234~mg/l	74	mg/l
309DAV	18060005	36.6468	-121.701	1/4/2011	Total suspended solids~Fixed~CEDEN~234~mg/l	1700	mg/l
309DAV	18060005	36.6468	-121.701	1/4/2011	Total suspended solids~Volatile~CEDEN~234~mg/l	180	mg/l
309DAV	18060005	36.6468	-121.701	1/4/2011	Total suspended solids~CEDEN~7~mg/l	1800	mg/l
309DAV	18060005	36.6468	-121.701	1/4/2011	Total dissolved solids~Fixed~CEDEN~234~mg/l	200	mg/l
309DAV	18060005	36.6468	-121.701	1/4/2011	Total dissolved solids~Volatile~CEDEN~234~mg/l	74	mg/l
309DAV	18060005	36.6468	-121.701	1/4/2011	Total dissolved solids~Dissolved~CEDEN~6~mg/l	270	mg/l
309GRN	18060005	36.3377	-121.205	1/25/2011	Total dissolved solids~Dissolved~CEDEN~49~mg/l	440	mg/l
309SAG	18060005	36.4863	-121.47	1/25/2011	Total dissolved solids~Dissolved~CEDEN~49~mg/l	470	mg/l
309SAC	18060005	36.5538	-121.548	1/25/2011	Total dissolved solids~Dissolved~CEDEN~49~mg/l	470	mg/l
309QUI	18060005	36.6096	-121.561	1/25/2011	Total dissolved solids~Dissolved~CEDEN~49~mg/l	570	mg/l
309SSP	18060005	36.629	-121.688	1/25/2011	Total dissolved solids~Dissolved~CEDEN~49~mg/l	470	mg/l
3098LA	18060005	36.7085	-121.749	1/26/2011	Total dissolved solids~Dissolved~CEDEN~49~mg/l	2090	mg/l

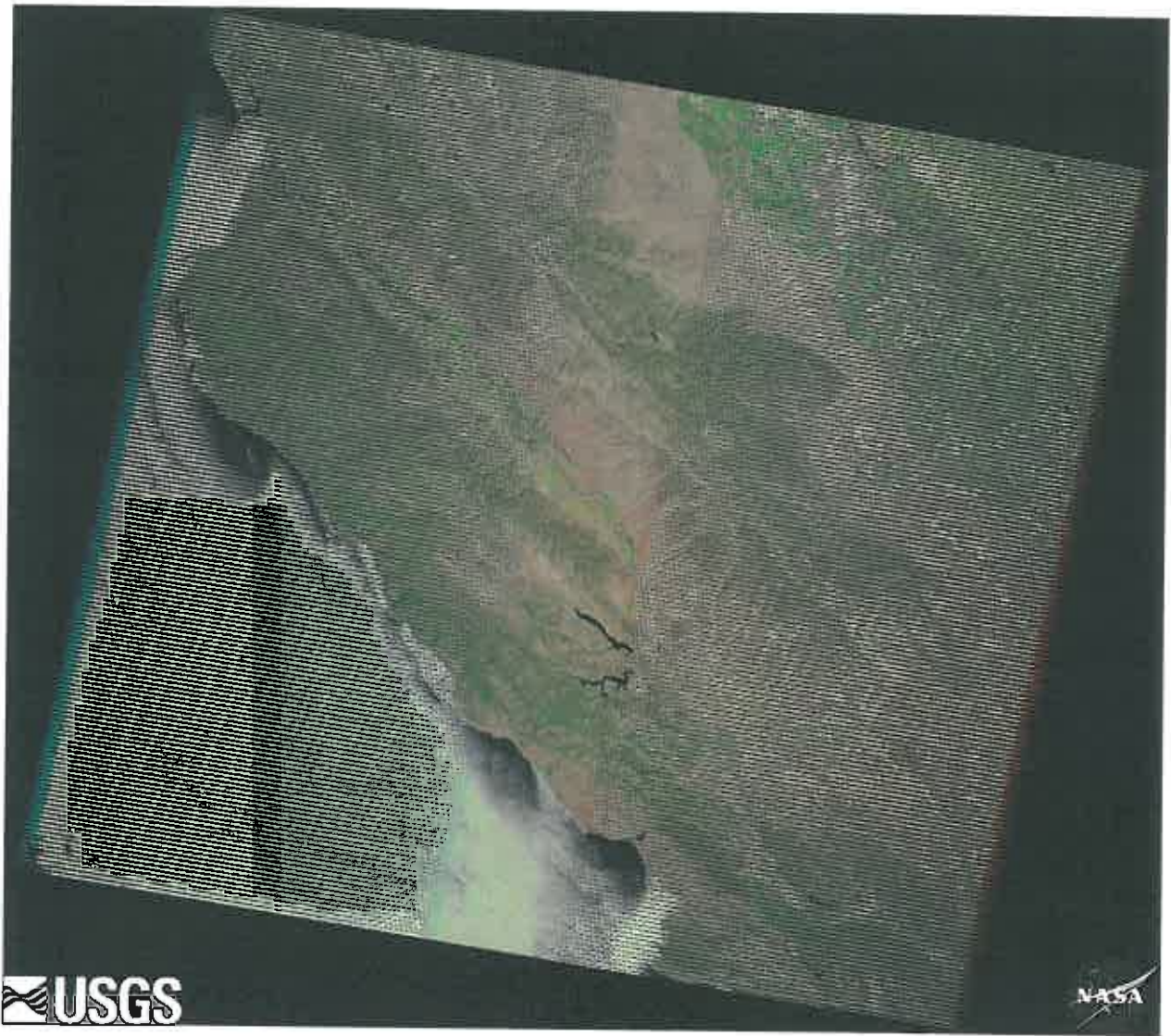
Appendix E

Map of TDS (in orange) and TSS (yellow) Stations



Appendix F

Landsat 7 Satellite Image Before Pozo Fire (August 15, 2010)



Appendix G

Landsat 7 Satellite Image After Pozo Fire (September 25, 2010)

